N72-23855

The Texas A&M University

Department of Physics
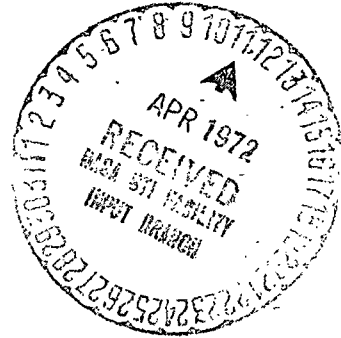College Station, Texas 77843

CASE FILE COPY

Report No. 3

Degree and Plane of Polarization of Multiple Scattered Light

I.   Homogeneous Cloud Layers

By George W. Kattawar and Gilbert N. Plass

Date of Issue: April 1, 1972

Grant No. NGR 44-001-117

Principal Investigators: Gilbert N. Plass

George W. Kattawar

Degree and Plane of Polarization of Multiple Scattered Light

I.   Homogeneous Cloud Layers

George W. Kattawar and Gilbert N. Plass

Department of Physics, Texas A&M University

College Station, Texas 77843

Abstract

The degree of polarization as well as the direction of the plane of polarization are calculated by a Monte Carlo method for homogeneous layers. Two solar zenith angles and a range of optical thicknesses up to 10 are considered. The results are compared with calculations for single scattered photons. For a given pair of incident and scattered directions, there are only two possible values for the direction of the plane of polarization differing by 90° for single scattering from spherical aerosols. The choice between these two values depends only on the sign of the element $\bar{M}$ in the first row and second column of the scattering matrix in the I, Q, U, V representation. In most cases there is little change in the direction of the plane of polarization when multiple scattering is taken into account, so that this quantity can usually be predicted from a very simple trigonometric relationship to good accuracy. Measurements of the direction of the plane of polarization at appropriately chosen angles provides information about the size distribution of the scattering centers.

Introduction

The solar radiation scattered by a planetary atmosphere is polarized. The degree of polarization depends on the solar angle and the angle of observation, the wavelength, the characteristics of the boundary, and the number density and distribution with height of the aerosols together with their single scattering phase function.

Various theoretical methods have been proposed for the numerical solution of radiative transfer problems. Unfortunately few of these have been applied to the problem of computing the polarization of radiation scattered from aerosols. The doubling principle described by van de Hulst and Grossman[1] has been used by Hansen[2] to obtain the polarization of the reflected light from cumulus and stratus clouds. Herman, Browning, and Curran[3] have calculated polarization values for light scattered from aerosols, but only for small optical thicknesses. Dave[4] has given both the polarization and ellipticity of the scattered radiation from particles with a size parameter of 10. No results have been reported by these methods for aerosols with large size parameters such as might be appropriate for nimbostratus or for ice crystal clouds.

The Monte Carlo method offers an entirely different approach to the solution of radiative transfer problems. There is no difficulty in using the phase functions which are highly peaked in the forward direction appropriate for large size scattering particles. Furthermore there is no difficulty in simulating realistic planetary atmospheres that have various components whose number density various with height. The Monte Carlo method has been described in general by Plass and Kattawar[5,6]; results for the polarization of the reflected and transmitted radiation have been given by Plass and Kattawar[6,7,8], Kattawar and Plass[9,10], and

Kattawar, Plass, and Adams[11]. Recently Mikhaylov and Nazaraliyev[12] have also described a Monte Carlo method for the calculation of the polarization. Unfortunately their method is wrong in some of its details and does not use as advanced a variance reduction techniques as ours. Specifically they incorrectly choose both the scattering and azimuthal angles from the wrong distributions; the scattering angles are modeled from the first component of the scattering matrix and the azimuthal angle is chosen from a uniform distribution. Actually both of these angles must be chosen from a bivariate distribution[6,9].

There are two different definitions of the degree of polarization. The first is known as the Rubenson definition:

$$P = -Q/I = (I_r - I_l)/(I_r + I_l), \tag{1}$$

where I_r and I_l are the intensities perpendicular and parallel to the incident plane. The four Stokes parameters are taken as (I, Q, U, V). The second definition is:

$$P = (Q^2 + U^2 + V^2)^{1/2}/I. \tag{2}$$

The angle χ which the direction of polarization (maximum intensity component) makes with the direction of the meridian plane containing the final photon direction is given by

$$\tan 2\chi = U/Q. \tag{3}$$

The polarizations given by the two definitions are identical when the sun is at the zenith, since U = V = 0. The polarization calculated from Eq. (1) is in general less than that obtained from Eq. (2) for other solar zenith angles. Our previous papers[8,9,10] which considered solar angles

away from the zenith used the Rubenson definition which gives the polarization measured along well defined axes. Dave[4] has pointed out that there would be more information in our results if we gave both the polarization calculated from Eq. (2) and the angle χ calculated from Eq. (3), since the polarization can then be calculated for any arbitrary orientation of the axes of the receiver. Dave[4] also states that we have been unable to obtain the angle χ by a Monte Carlo method. Actually χ is easily obtained by the Monte Carlo method and in most cases is determined with a relatively small probable error. All of the values for the polarization given in this paper are obtained from Eq. (2). Both P and χ are presented here for homogeneous layers of scattering centers representing continental haze, nimbostratus, and ice crystal clouds. Optical thicknesses up to 10 are considered for both a high and low solar elevation. For comparison the single scattered results are given in each case.

Method

The scattering matrix for three different size distributions was calculated exactly from the Mie theory[13] for a wavelength of 0.7μ. The first distribution for a continental haze (haze C) proposed by Deirmendjian[14] assumes spherical water droplets with an index of refraction of 1.33. The particle concentration is constant when $0.03\mu < r < 0.1\mu$ and is proportional to r^{-4} when $r > 0.1\mu$. The second distribution, known as the nimbostratus model, assumes fairly large water droplets. The particle concentration is proportional to $r^6 \exp(-0.5r)$ and the modal radius is 12μ.

The third distribution is hopefully representative of some ice

crystal clouds. Although the size distribution for ice crystals in clouds is not so well known as that for water droplets, the average size of the ice crystals under many conditions is possibly considerably larger. Their shapes are irregular and usually far from spherical. However, we represent them by spherical particles, so that the single scattering function may be computed from the Mie theory. This assumption may introduce unknown errors in various elements of the scattering matrix. Until measured values of the elements of the scattering matrix are available, this assumption must suffice. The assumed size distribution is:

$$n(r) = Ar^5 \exp(0.1)r, \qquad (4)$$

where A is a constant. The modal radius for this distribution is 50μ. The value of the parameter $x = 2\pi r/\lambda$, where r is the particle radius and λ is the wavelength, is 449 at λ = 0.7μ when r = 50μ. The integration over the size distribution was continued to x = 1800, which corresponds to r = 200μ. An efficient program is essential when x values become as large as this.[5] The index of refraction of ice was taken as 1.310 at this wavelength.

All the components of the scattering matrix were calculated in this ·manner for each of the three models and were used as input data for the Monte Carlo calculation. Since the Monte Carlo code has been described previously,[5,6] only a brief description is given here. The four component Stokes vector is obtained after each scattering event from the vector before scattering from an appropriate matrix transformation. This matrix involves the four independent components of the scattering matrix previously calculated from Mie theory. Both the scattering angle and the azimuthal angle of the photon direction after scattering are chosen from

approximate distributions. However, the weight associated with each photon is multiplied by an appropriate factor, so that the final result is exactly the same as though the angles had been chosen from the correct bivariate distribution.

Collisions are forced so that the photon never leaves the atmosphere; again the weight associated with the photon is adjusted so that the correct result is obtained. The photons are followed until their weight is so small that they make a negligible contribution to any of the detectors. It should be emphasized that the exact three-dimensional path of the photon is followed in the Monte Carlo method; the only averaging in the method is at the detectors, where the radiance is averaged over finite intervals of solid angle.

In a Monte Carlo method a compromise must always be made in the choice of the angular intervals over which the results are averaged. If the intervals are too large, the angular variation of the function is not obtained. On the other hand, if they are too small, the statistical fluctuations may become large due to insufficient counts. For the present calculations, we chose intervals of 0.1 for the cosine of the zenith or nadir angle as a reasonable compromise. In all cases the calculated value is a true average over the interval; no uncertainties are introduced into the calculation by this choice. All four components of the Stokes vector are calculated for each interval. A true average value is obtained for each of these quantities. The polarization and χ are then calculated from Eqs. (2) and (3) for each angular interval.

Single Scattering

The plane of polarization after single scattering of initially

unpolarized light is determined entirely by the direction of the inci-
dent and scattered photon and the sign of the element M^- in the scatter-
ing matrix. Thus for a given incident and scattered direction, the
angle χ can have only two values differing by $\pi/2$ for scattering from
any spherical aerosol. When the Stokes vector is chosen as (I, Q, U, V),
the scattering matrix for spherical particles has the form

$$R = \begin{vmatrix} M^+ & M^- & 0 & 0 \\ M^- & M^+ & 0 & 0 \\ 0 & 0 & S_{21} & -D_{21} \\ 0 & 0 & D_{21} & S_{21} \end{vmatrix} , \qquad (5)$$

where the four independent elements are written as M^+, M^-, S_{21}, D_{21}.
The Stokes parameters for initially unpolarized light after single
scattering described by the matrix of Eq. (5) are: $I = M^+$; $Q = M^- \cos 2i_2$; $U = M^- \sin 2i_2$; $V = 0$, when i_2 is the angle between the scatter-
ing plane and the meridian plane containing the final photon direction
and the zenith direction (see Chandrasekhar[15], p. 39). Thus after
scattering, $U/Q = \tan 2i_2$. The following relation holds in spherical
trigonometry:

$$\cot i_2 = (\sin \theta \cot \theta_o - \cos \theta \cos \phi)/\sin \phi, \qquad (6)$$

where θ_o and θ are the polar angles for the initial and scattered photon
directions and ϕ is the azimuthal angle between the initial and scattered
meridian planes.

Thus it follows from Eq. (3) and the ratio of Stokes parameters,
U/Q, after the scattering calculated from the matrix of Eq. (5) that

$$\tan 2 \chi = U/Q = \tan 2i_2, \qquad (7)$$

$$\chi = i_2 \pm \frac{1}{2} n \pi.$$

The angle i_2 $(0 < i_2 < \pi)$ is determined uniquely for each scattering event by Eq (6) from the angles which describe the photon path before and after the collision. From Eqs. (6) and (7) the angle of the plane of polarization χ is given by

$$\chi = \tan^{-1} [\sin \theta /(\sin \theta \cot \theta - \cos \theta \cos \phi)] \pm \frac{1}{2} n \pi, \quad (8)$$

where n is an integer and $-\frac{1}{2}\pi < \chi < \frac{1}{2} \pi$. Thus χ is determined for single scattering of unpolarized light from the angles which describe the photon path before and after the collision except for an arbitrary factor of $\frac{1}{2} \pi$. There are only two possible values of χ for a given set of initial and final photon directions regardless of the values of the elements of the scattering matrix. The sign of the matrix element $\bar{M}$ determines which one of the two possible values of χ is appropriate, as is shown in Table I. The first column shows a possible range for the angle i_2. The second and third columns show the signs of Q and U for the sign of the matrix element $\bar{M}$ shown in the fourth column. The matrix element $\bar{M}$ is always negative for Rayleigh scattering. The allowed range of χ is given in the fifth column.

If we consider, for example, a smooth variation of the angle θ_o holding the other scattering angles fixed, then for Rayleigh scattering $(\bar{M} < 0)$ the plane of maximum polarization varies smoothly. The angle χ also varies continuously, except that when it reaches the end of its range, i.e. 90°, it jumps to a value at the other end of the range, -90° or vice versa. There is no corresponding jump in the position of the plane of maximum polarization; it continues to rotate in a continuous

manner in space as χ passes through the value $\pm 90^{\circ}$. On the other hand with aerosol scattering, $\bar{M}$ may change sign one or more times as θ_o varies. When this occurs, both Q and U change sign and χ (which may have any value in its range when this happens) discontinuously changes its value by $\pm 90^{\circ}$; the actual plane of polarization in space also changes discontinuously by 90°. However, at the particular angle for which $\bar{M} = 0$, Q = 0 and U = 0 so that the two components of the scattered radiation have equal magnitude; the direction of maximum intensity and thus the angle χ cannot be defined at such an angle.

In summary, the angle χ is determined for single scattering from a distribution of spherical particles entirely by the initial and final photon directions except for a possible factor of 90°. This latter factor is determined by the sign of the element $\bar{M}$ of the phase matrix. Thus χ can readily be obtained from Eq. (8) from the knowledge of the angles which define the scattering event, θ, θ_o and ϕ. This fact does not seem to have been mentioned in the literature previously. It is especially important since χ (or the ratio of U to Q) is usually a slowly varying function of optical depth. Thus a good approximation can often be obtained for a finite optical depth from the result valid for single scattering.

Polarization of Reflected Photons

The results of the Monte Carlo calculations of the polarization and the direction of polarization are presented in this section for reflected photons scattered according to each of the three models already discussed: haze C, nimbostratus, and ice crystal. The definition of polarization given by Eq. (2) is used throughout this paper. The following two values for the cosine of the angle from the incident solar direction to the zenith were chosen: $\mu_o = 0.81915$ ($\theta = 35^{\circ}$) and $\mu_o = 0.1$ ($\theta = 84.26^{\circ}$).

These two angles were chosen to represent moderately high and low solar elevations. The case of the sun at the zenith is not interesting for the present purposes since the polarization obtained from Eqs. (1) and (2) is the same and χ can be obtained from elementary considerations.

The Monte Carlo results are presented as a function of the cosine of the angle between the direction of observation and the nadir, μ, and of the azimuthal angle, ϕ, measured from the incident plane. The following intervals were chosen: $\Delta\mu = 0.1$ and $\Delta\phi = 30°$; the Monte Carlo results were averaged over this range of angles in each case. The values given are a true average over the indicated range. For some applications narrower angular ranges are required; in these cases the Monte Carlo method is probably not suited. However, in many cases averages over intervals of this order provide an ideal presentation of the angular variation of a complicated function. The models of the various types of clouds are only approximations so that the calculated values can never be expected to agree in all details with measurements for a given experimental situation.

The polarization is given in Figs. 1 - 3 for $\mu_o = 0.81915$ for optical thicknesses of the scattering layer, τ, of 0.01, 0.1, 1, and 10. The results are given for the haze C, nimbostratus, and ice crystal models. In Fig. 1 the solar horizon is on the left, the nadir at the center, and the antisolar horizon is at the right of the figure. The polarization of a single scattered photon is also shown for comparison. This was calculated from Eq. (2) and the scattering matrix. The result was averaged over the same ϕ intervals as were used in the Monte Carlo calculation so that the two results could be compared directly.

The single scattered polarization shows a relatively sharp maximum

at the rainbow angle for the nimbostratus and ice crystal models, but not

for haze C. The ice crystal model shows a high value of the polarization

in the region midway between the nadir and the solar horizon at all

angles ϕ.

The Monte Carlo results for $\tau = 0.01$ show good agreement in general

with the single scattered polarization curves. As τ increases, the polari-

zation decreases in general as indicated on these figures. The position

of the symbol for a Monte Carlo result within one μ interval has no

significance; the symbols were moved horizontally within an interval to

distinguish them better visually when they were close together. In some

cases it was impossible to plot all of the symbols due to overlap. In

this case the missing symbol is very close to the one for the next lowest

τ value for the same model. The decrease in the polarization with in-

creasing τ in each case is shown in the figure.

The polarization for other ϕ ranges is shown in Figs. 2 and 3. The

polarization tends to increase as ϕ increases toward 90° and then to de-

decrease again as ϕ approaches 180° (except for the large polarization

values near the rainbow angles). When ϕ is near 90° the scattering angle

for single scattering from the solar direction into the direction of ob-

servation also tends to be of the order of 90°, a region where the single

scattered photons often have a relatively large polarization.

The direction of the plane of polarization, χ, is shown for these

same cases in Figs. 4 - 6. The value of χ for single scattered photons

is shown for each of the three models. This result was averaged over the

same ϕ intervals as were used in the Monte Carlo calculations. When only

one curve is shown the values for the other models are the same within

the accuracy of the plot. It should be remembered that the range of χ

is taken as $-90° < \chi < 90°$; thus, when the value of χ is increasing and

reaches $90°$, it then changes to $-90°$. The apparent jump in the curve

does not correspond to a discontinuity in any physical parameter, since

the plane of polarization is rotating continuously. The curves shown

here would be continuous if they were wrapped arount the surface of a

cylinder with its axis parallel to the μ direction so that the χ values

for $90°$ and $-90°$ became joined.

For the range $0° < \phi < 30°$, the two allowed values of χ are near

$10°$ and $-80°$. The curve for haze C is near $-80°$ from the solar horizon to

the nadir (where in all cases the value jumps to the negative of its

previous value as the nadir is crossed because of the symmetries of the

problem). The value of the matrix element $\bar{M}$ changes sign for the ice

crystal model near $\mu = 0.2$ so that χ changes rapidly from the value $10°$

to $-80°$. A similar change occurs from the nimbostratus model near

$\mu = 0.34$. If we were plotting the χ value for a particular value of

ϕ, the χ curve would jump discontinuously from one of the allowed values

to the next when $\bar{M}$ changes sign. Because our values of U and Q were

averaged over $0° \le \phi \le 30°$, the resulting curve for χ has a transition

region which may be relatively sharp or broad depending upon whether the

matrix element $\bar{M}$ changes sign at nearly the same value of μ or over a

broad range of values of μ as the scattering angle takes on all possible

values consistant with the range of values of μ and ϕ considered. Ex-

amples of curves with broader transition regions are shown in Fig. 4 in

the range $150° < \phi < 180°$. When ϕ is near $90°$, χ is nearly the same for

each of the three models. In most cases the values of χ show no appre-

ciable variation with τ. The values for larger τ were not plotted since

they showed greater fluctuations and no discernable trend.

The polarization of the reflected photons for $\mu_o = 0.1$ ($\beta = 84.26°$) is shown in Figs. 7-9. These curves give typical results for a low solar elevation. In the incident plane (Fig. 7) the high polarization for the nimbostratus and ice crystal models near the rainbow angle is evident. The polarization is usually high at this angle even for $\tau = 10$. The polarization is small when $0° < \phi < 30°$ and when $30° < \phi < 60°$ compared to the much larger values for these ranges when $\mu_o = 0.81915$. The polarization is relatively large in most cases when $60° < \phi < 120°$.

The direction of the plane of polarization when $\mu_o = 0.1$ is shown in Figs. 10-12. The differences between these curves and those for the higher solar elevation are interesting. For example, when $0° < \phi < 30°$ the curves for the nimbostratus and ice crystal models break away from the curve for the haze C model near $\mu = 0.9$; this occurs at a much smaller μ value when $\mu_o = 0.81915$. This behavior is determined by the sign of the matrix element $\bar{M}$ for the particular scattering angles allowed. Another interesting example is when $60° < \phi < 90°$ (Fig. 12); the χ values for the haze C and ice crystal models are nearly the same over the entire range of μ, while the curve for the nimbostratus model is different from the others.

Polarization of the Transmitted Photons

The polarization of the transmitted photons as a function of the cosine of the zenith angle μ, when $\mu = 0.81915$ is shown in Figs. 13 - 15. The direct solar beam is defined to have $\phi = 0°$ and thus occurs at the point $\mu = 0.81915$ on the left hand side of Fig. 13. The solar horizon is on the left side of the figure, the zenith is at the center, and the anti-

solar horizon is at the right. The polarization is given for transmission through homogeneous layers with τ = 0.01, 0.1, 1, and 10. In general, as the single scattering angle approaches 90°, the polarization becomes larger; thus the polarization is often greater when 90° < ϕ < 180° than when 0° < ϕ < 90°. The polarization is less than 0.25 in all cases when 0° < ϕ < 60° and is small for the range 60° < ϕ < 90° except close to the horizon.

The direction of the plane of polarization for μ_o = 0.81915 is shown in Figs. 16 - 18. This sequence of curves is instructive. When 0° < ϕ < 30°, χ changes rapidly as μ increases from 0.6 to 1.0 (Fig. 16). When the scattering angle is near 0°, the matrix element $\overline{M}$ undergoes several sign changes over a relatively small range of μ. When 30° < ϕ < 60° (Fig. 17), χ is a relatively slowly varying function of μ; The haze C model gives one curve, while the nimbostratus and ice crystal models follow nearly identical curves displaced by 90° from that for the haze C model. In this case $\overline{M}$ has a negative sign throughout the entire range for the haze C model and a positive sign for the nimbostratus and ice crystal models. Finally when 60° < ϕ < 90°, χ is also a relatively slowly varying function of μ; in this case as μ increases from the value zero, the curves for the nimbostratus and ice crystal models break away from the haze C curve when the sign of $\overline{M}$ changes from negative to positive. Similarly when ϕ > 90°, the curves for the nimbostratus and ice crystal models also break away from the curve for the haze C model at a particular value of μ in each case; this occurs at the point where $\overline{M}$ changes sign as the scattering angle varies.

The polarization for low solar elevation (μ_o = 0.1) is shown in

Figs. 19 - 21. The photons observed in the solar direction (μ = 0.1,

left-hand side of Fig. 19) are unpolarized when τ is small; however, when

τ = 10 virtually all of the photons observed in this direction have under-

gone multiple scattering and the polarization increases to respectable

values in some cases. This is one of the few cases where the polarization

increases as the optical depth increases. In general the polarization is

small in the incident plane from the solar direction up to the zenith and

is large from the zenith most of the way down to the anti-solar horizon.

When ϕ is near 90°, the polarization is large over a considerable range of

angles, particularly for the haze C and ice crystal models. One of the

most striking changes in the polarization as the sun moves from a small

to a large solar zenith angle occurs in the region of the sky near the

zenith; when 60° < ϕ < 120°, the polarization is small for small solar

zenith angle (Fig. 15) and is often fairly large for large solar zenith

angle (Fig. 21). The reason for this variation is connected with the

small single scattering angle in the former case and a scattering angle

near 90° in the latter case.

The direction of the plane of polarization for μ_o = 0.1 is given in

Figs. 22 - 24. These curves are very different from the corresponding

curves for μ_o = 0.81915. When 0° < ϕ < 30°, χ is a rapidly varying

function of μ near the solar direction (μ_o = 1). From 0.2 < μ < 0.9 the

haze C model has one set of values of χ, while the nimbostratus and ice

crystal models cluster around the other possible set. Other groupings

of the values for the different models are seen for different ranges of

ϕ. For example, all three models give the same χ value when 90° < ϕ < 120°;

on the other hand, for 60° < ϕ < 90°, the haze C and ice crystal models

give one set of χ values while the nimbostratus model follows the other possible χ curve over most of the range in μ.

Conclusions

Useful data has been obtained from a Monte Carlo method about the polarization as well as the direction of the plane of polarization for homogeneous layers corresponding to the haze C, nimbostratus, and ice crystal models. Results for various optical thicknesses and two solar zenith angles show the variation with these parameters.

For single scattering the direction of the plane of polarization is completely determined by the direction of the incident and scattered photons and the sign of the element $\bar{M}$ of the scattering matrix. In most cases the direction of the plane of polarization does not change appreciably with the optical thickness of the scattering layer and thus the same conclusion applies approximately when multiple scattering is taken into account.

A measurement of the direction of the plane of polarization of either reflected or transmitted photons at carefully selected viewing angles can give a great deal of information about the nature of the scattering centers. These measurements are not critical since only two values of χ differing by 90^0 are possible for a given solar angle and viewing direction. For example when $\mu_o = 0.1$, one or two measurements of χ for the transmitted photons would distinguish the three models discussed here. A measurement in the range $30° < \phi < 60°$ and $\mu < 0.8$ would show that the particle size distribution was closer to the haze C model than the other two considered here if the value of χ were on the upper

curve of Fig. 23. If the value were on the lower curve in this range, an additional measurement should be made in the range $60° < \phi < 90°$ and $\mu < 0.6$. If the χ value is near $0°$ then the nimbostratus model is appropriate, while if the value is near $\pm 90°$, then the ice crystal model is valid.

Although this example is for a particular solar zenith angle and for transmitted photons, similar considerations can be applied at other solar angles as well as for the reflected photons. Of course, in practice it might be necessary to allow for more size distributions than were considered here, but there will still be regions where the measured values of χ are $90°$ apart for any pair of models. These regions occur when the matrix element $\bar{M}$ has opposite sign for the two models over an appropriate range of scattering angles and the corresponding range of viewing angles.

REFERENCES

1. H. C. van de Hulst and K. Grossman, "Multiple Light Scattering in Planetary Atmospheres" in The Atmosphers of Venus and Mars, J. C. Brandt and M. B. McElroy, Eds. (Gordon and Breach, New York, 1968), pp. 35-55.

2. J. E. Hansen, J. Atmos. Sci 28, 1400 (1971).

3. B. M. Herman, S. R. Browning, R. J. Curran, J. Atmos. Sci. 28, 419 (1971).

4. J. V. Dave, Appl. Opt. 9, 2673 (1970).

5. G. N. Plass and G. W. Kattawar, Appl. Opt. 7, 415 (1968).

6. G. N. Plass and G. W. Kattawar, J. Atmos. Sci. 28, 1187 (1971).

7. G. N. Plass and G. W. Kattawar, Appl. Opt. 8, 2489 (1969).

8. G. N. Plass and G. W. Kattawar, Appl. Opt. 9, 1122 (1970).

9. G. W. Kattawar and G. N. Plass, Appl. Opt. 7, 1519 (1968).

10. G. W. Kattawar and G. N. Plass, Appl. Opt. 10, 74 (1971).

11. G. W. Kattawar, G. N. Plass, and C. N. Adams, Astroph. J. 170, 371 (1971).

12. G. A. Mikhaylov and M. A. Nazaraliyev, Izv., Atmos. Oceanic Phys. 7, 254 (English), 377 (Russian) (1971).

13. G. W. Kattawar and G. N. Plass, Appl. Opt. 6, 1377 (1967).

14. D. Deirmendjian, Appl. Opt. 3, 187 (1964).

15. S. Chandrasekhar, Radiative Transfer (Dover Publications, Inc., New York, 1960).

Table I. Angle of Plane of Polarization

i_2	Q	U	M$_-$	χ
$0°<i_2<45°$	−	−	−	$-90°<\chi<-45°$
$45°<i_2<90°$	+	−	−	$-45°<\chi<0°$
$90°<i_2<135°$	+	+	−	$0°<\chi<45°$
$135°<i_2<180°$	−	+	−	$45°<\chi<90°$
$0°<i_2<45°$	+	+	+	$0°<\chi<45°$
$45°<i_2<90°$	−	+	+	$45°<\chi<90°$
$90°<i_2<135°$	−	−	+	$-90°<\chi<-45°$
$135°<i_2<180°$	+	−	+	$-45°<\chi<0°$

LEGENDS FOR FIGURES

Fig. 1. Polarization of reflected radiation as a function of the cosine of the nadir angle, μ. The cosine of the solar zenith angle μ_o = 0.81915. The results have been averaged over the azimuth angle ϕ measured from the incident plane over a range $0^o < \phi < 180^o$ on the right side. The solar horizon is on the left side of the figure, the nadir at the center, and the antisolar horizon on the right side. The surface albedo is taken as zero in all cases. Results are given for single scattering and for multiple scattering with optical thickness τ = 0.001, 0.1, 1, 10 for the haze C, nimbostratus, and ice crystal models.

Fig. 2. Polarization of reflected radiation for $30^o < \phi < 60^o$ and $120^o < \phi < 150^o$ and μ_o = 0.81915.

Fig. 3. Polarization of reflected radiation for $60^o < \phi < 120^o$ and μ_o = 0.81915.

Fig. 4. Plane of polarization χ of reflected radiation as a function of μ for μ_o = 0.81915 for $0^o < \phi < 30^o$ and $150^o < \phi < 180^o$. Results are given for single scattering and for multiple scattering with τ = 0.01 and 0.1.

Fig. 5. Plane of polarization of reflected radiation for $30^o < \phi < 60^o$ and $120^o < \phi < 150^o$ and μ_o = 0.81915.

Fig. 6. Plane of polarization of reflected radiation for $60^o < \phi < 120^o$ and μ_o = 0.81915

Fig. 7. Polarization of reflected radiation for μ_o = 0.1 and $0^o < \phi < 30^o$ and $150^o < \phi < 180^o$.

Fig. 8. Polarization of reflected radiation for $30^o < \phi < 60^o$ and $120^o < \phi < 150^o$ and μ_o = 0.1.

Fig. 9. Polarization of reflected radiation for $60^o < \phi < 120^o$ and μ_o = 0.1.

Fig. 10. Plane of polarization of reflected radiation for $0^o < \phi < 30^o$ and $150^o < \phi < 180^o$ and μ_o = 0.1.

Fig. 11. Plane of polarization of reflected radiation for $30^o < \phi < 60^o$ and $120^o < \phi < 150^o$ and μ_o = 0.1.

Fig. 12. Plane of polarization of reflected radiation for $60^o < \phi < 120^o$ and μ_o = 0.1.

Fig. 13. Polarization of transmitted radiation as a function of the zenith angle, μ for $0^{\circ} < \phi < 30^{\circ}$ and $150^{\circ} < \phi < 180^{\circ}$ and $\mu_{o} = 0.81915$. The solar horizon is on the left side of the figure, the zenith at the center, and the antisolar horizon on the right side. The direction of the unscattered solar photons is between the solar horizon and the zenith.

Fig. 14. Polarization of transmitted radiation for $30^{\circ} < \phi < 60^{\circ}$ and $120^{\circ} < \phi < 150^{\circ}$ and $\mu_{o} = 0.81915$.

Fig. 15. Polarization of transmitted radiation for $60^{\circ} < \phi < 120^{\circ}$ and $\mu_{o} = 0.81915$.

Fig. 16. Plane of polarization of transmitted radiation for $0^{\circ} < \phi < 30^{\circ}$ and $150^{\circ} < \phi < 180^{\circ}$ and $\mu_{o} = 0.81915$.

Fig. 17. Plane of polarization of transmitted radiation for $30^{\circ} < \phi < 60^{\circ}$ and $120^{\circ} < \phi < 150^{\circ}$ and $\mu_{o} = 0.81915$.

Fig. 18. Plane of polarization of transmitted radiation for $60^{\circ} < \phi < 120^{\circ}$ and $\mu_{o} = 0.81915$.

Fig. 19. Polarization of transmitted radiation for $0^{\circ} < \phi < 30^{\circ}$ and $150^{\circ} < \phi < 180^{\circ}$ and $\mu_{o} = 0.1$.

Fig. 20. Polarization of transmitted radiation for $30^{\circ} < \phi < 60^{\circ}$ and $120^{\circ} < \phi < 150^{\circ}$ and $\mu_{o} = 0.1$.

Fig. 21. Polarization of transmitted radiation for $60^{\circ} < \phi < 120^{\circ}$ and $\mu_{o} = 0.1$.

Fig. 22. Plane of polarization of transmitted radiation for $0^{\circ} < \phi < 30^{\circ}$ and $150^{\circ} < \phi < 180^{\circ}$ and $\mu_{o} = 0.1$.

Fig. 23. Plane of polarization of transmitted radiation for $30^{\circ} < \phi < 60^{\circ}$ and $120^{\circ} < \phi < 150^{\circ}$ and $\mu_{o} = 0.1$.

Fig. 24. Plane of polarization of transmitted radiation for $60^{\circ} < \phi < 120^{\circ}$ and $\mu_{o} = 0.1$.
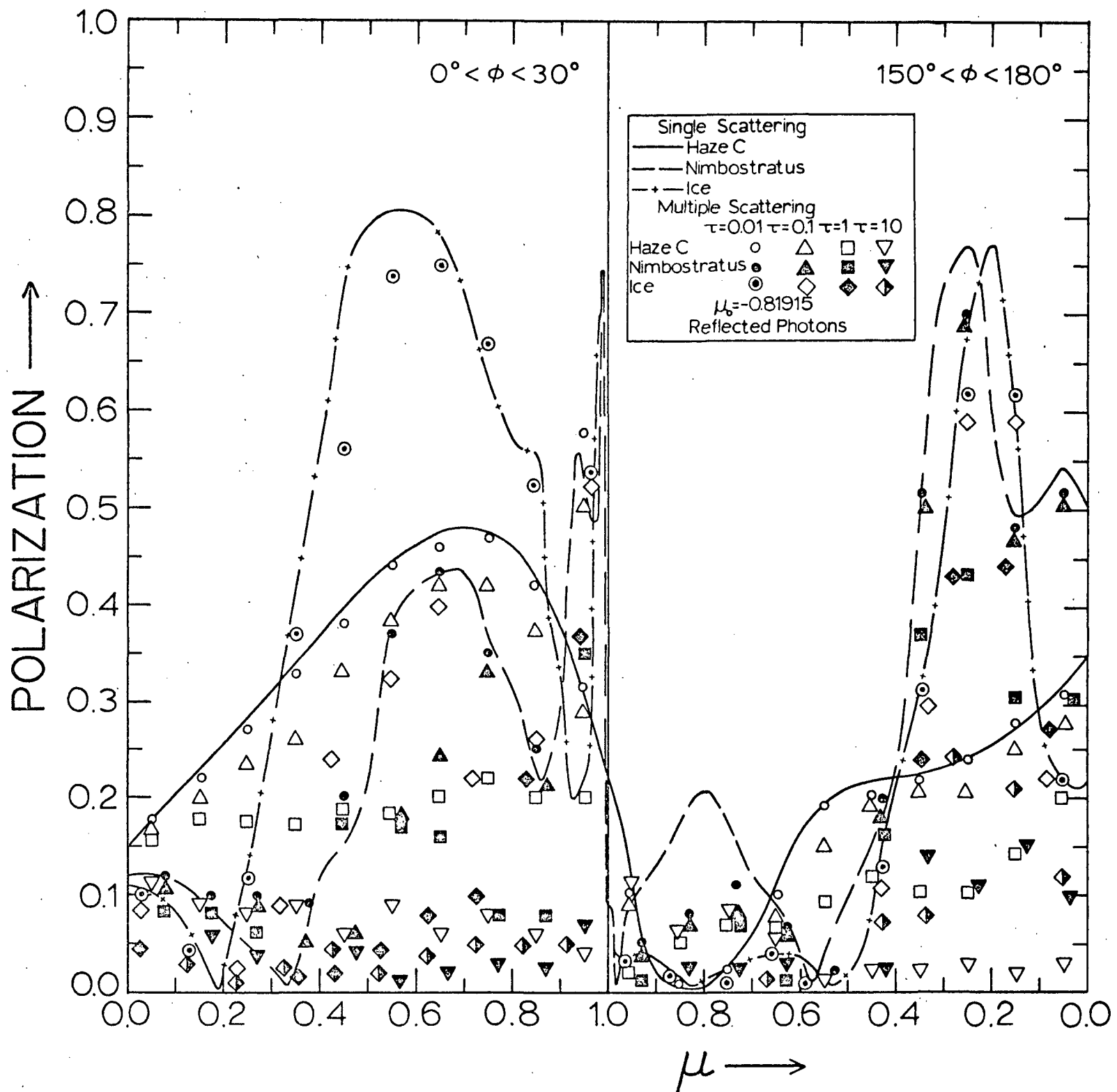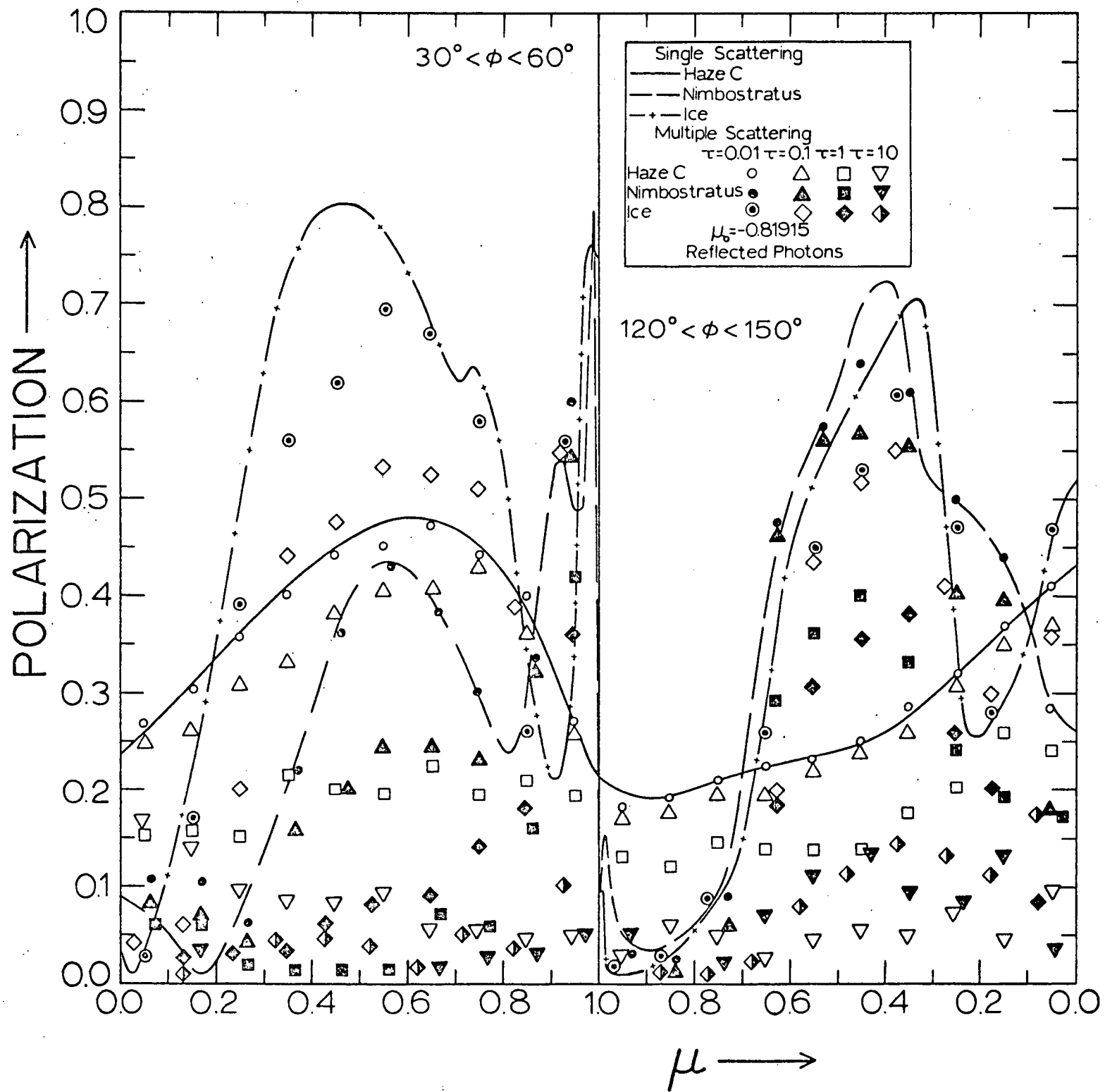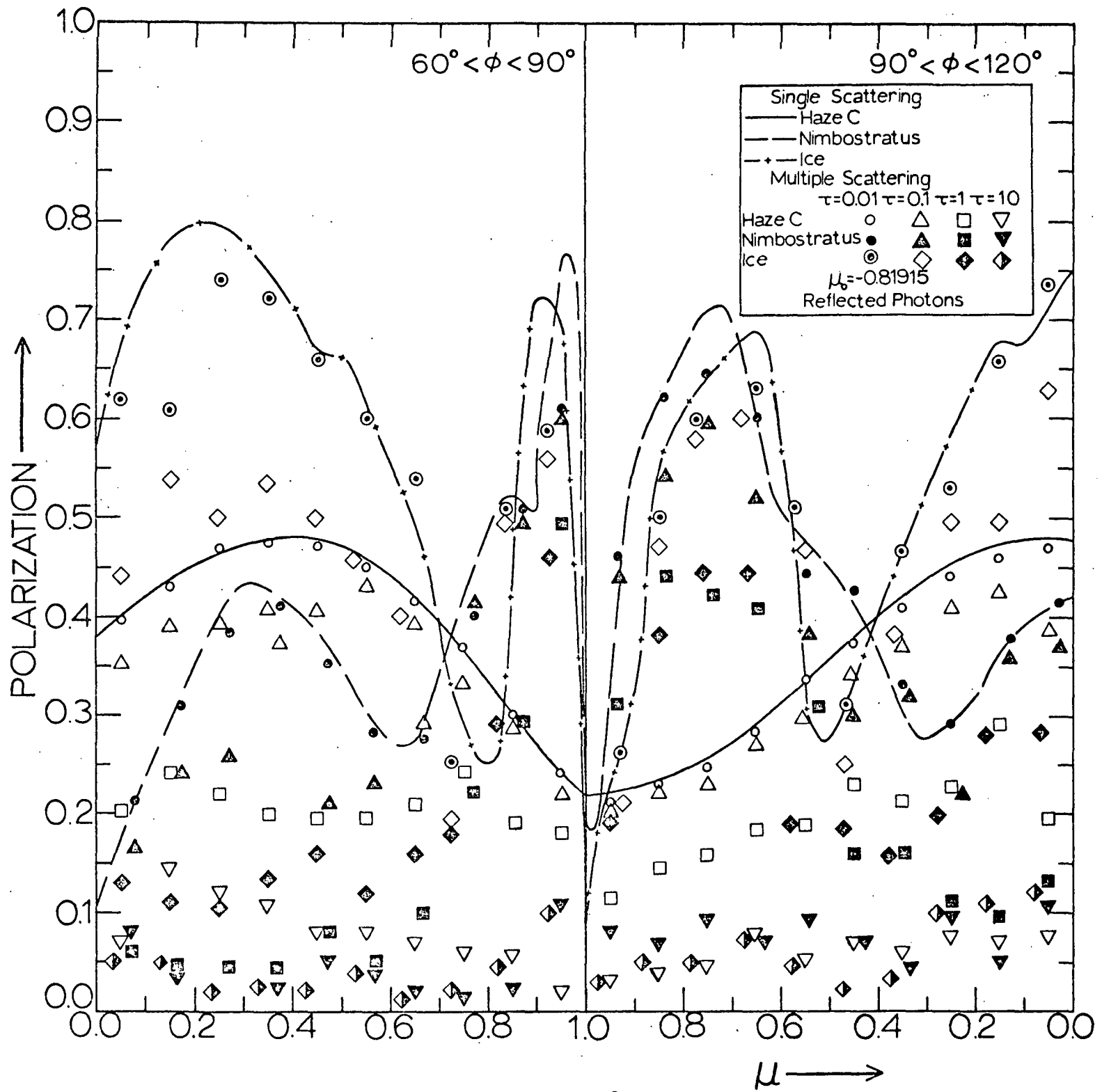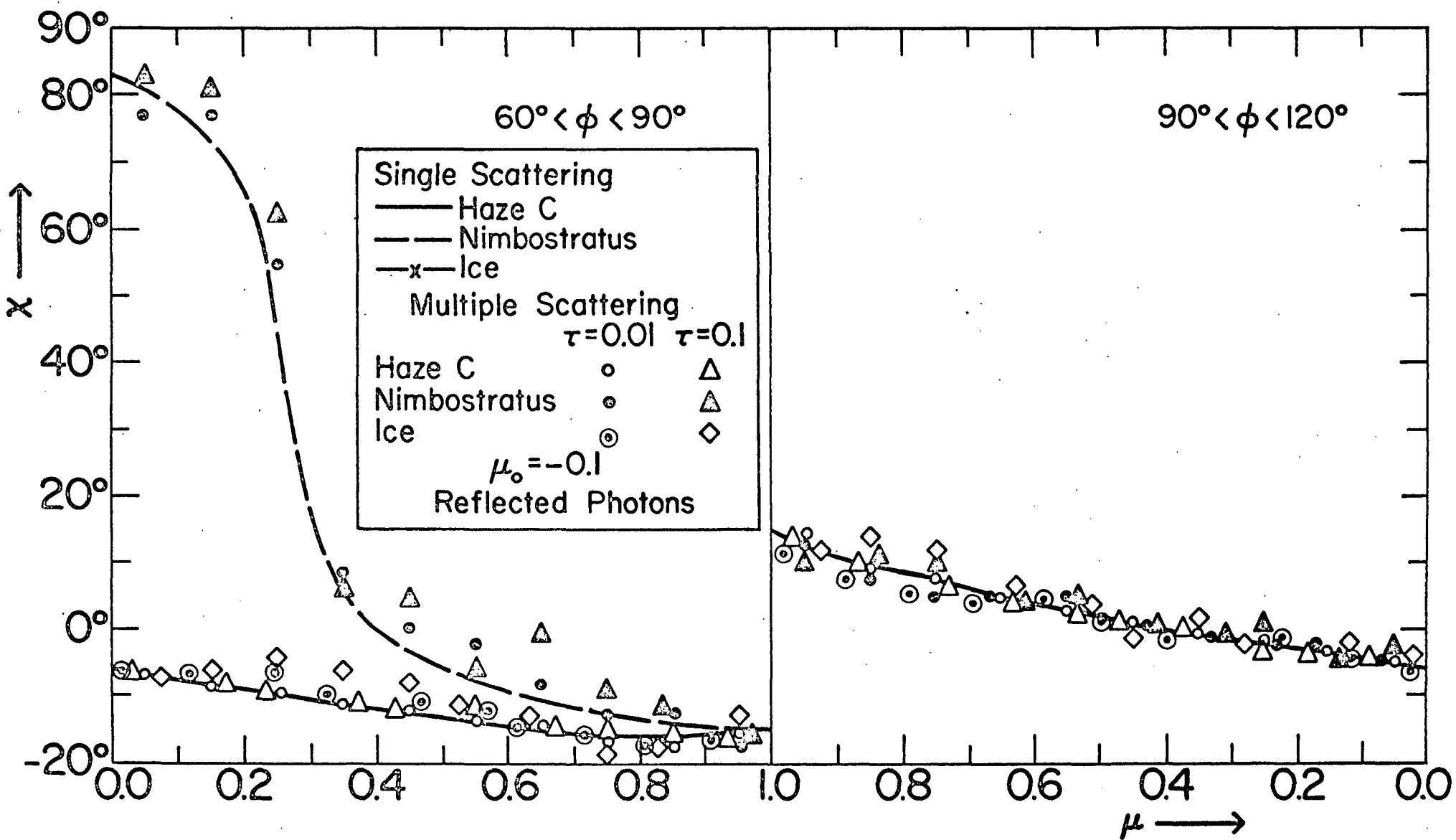
Fig. 1

Fig. 2

Fig. 3
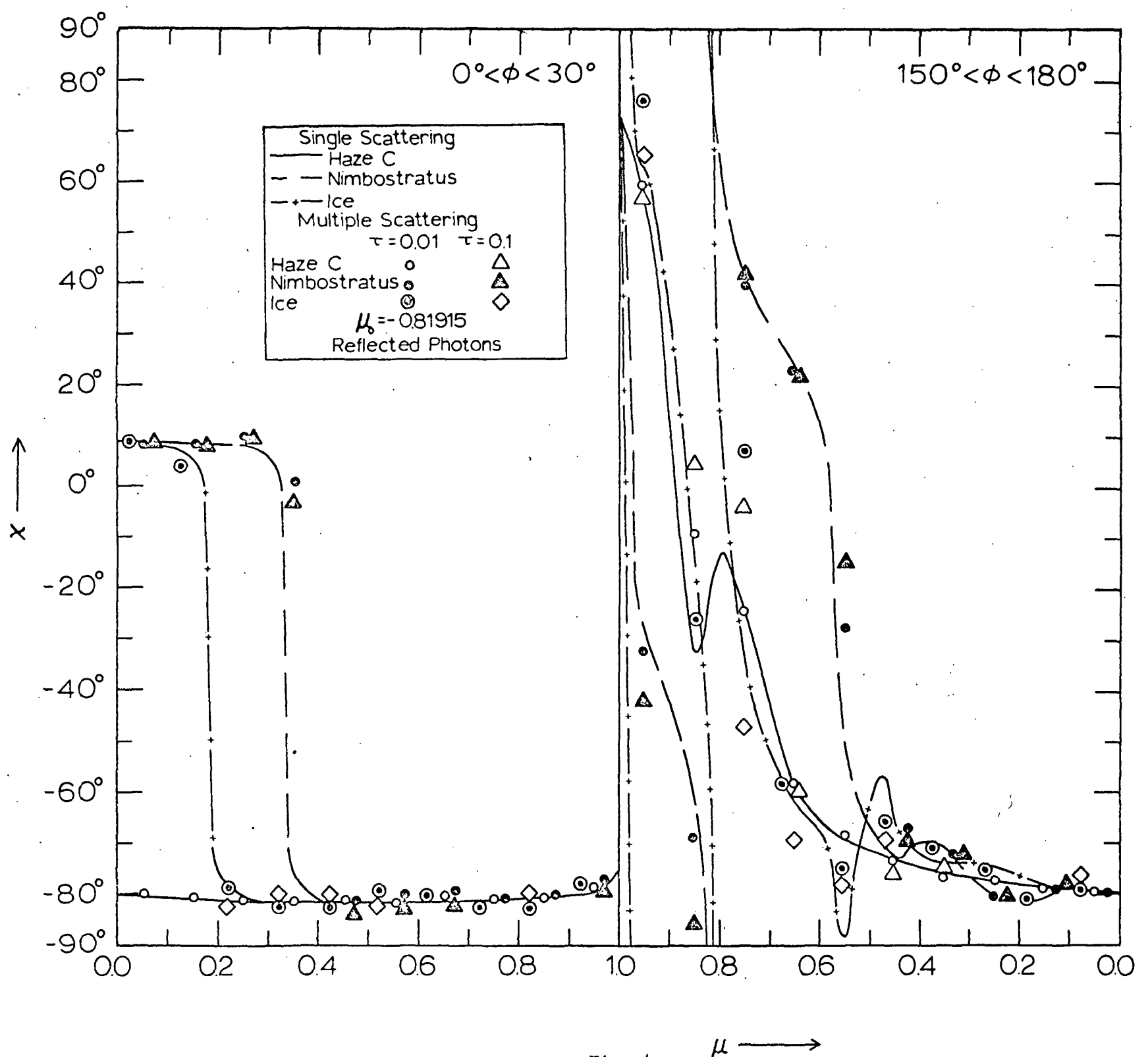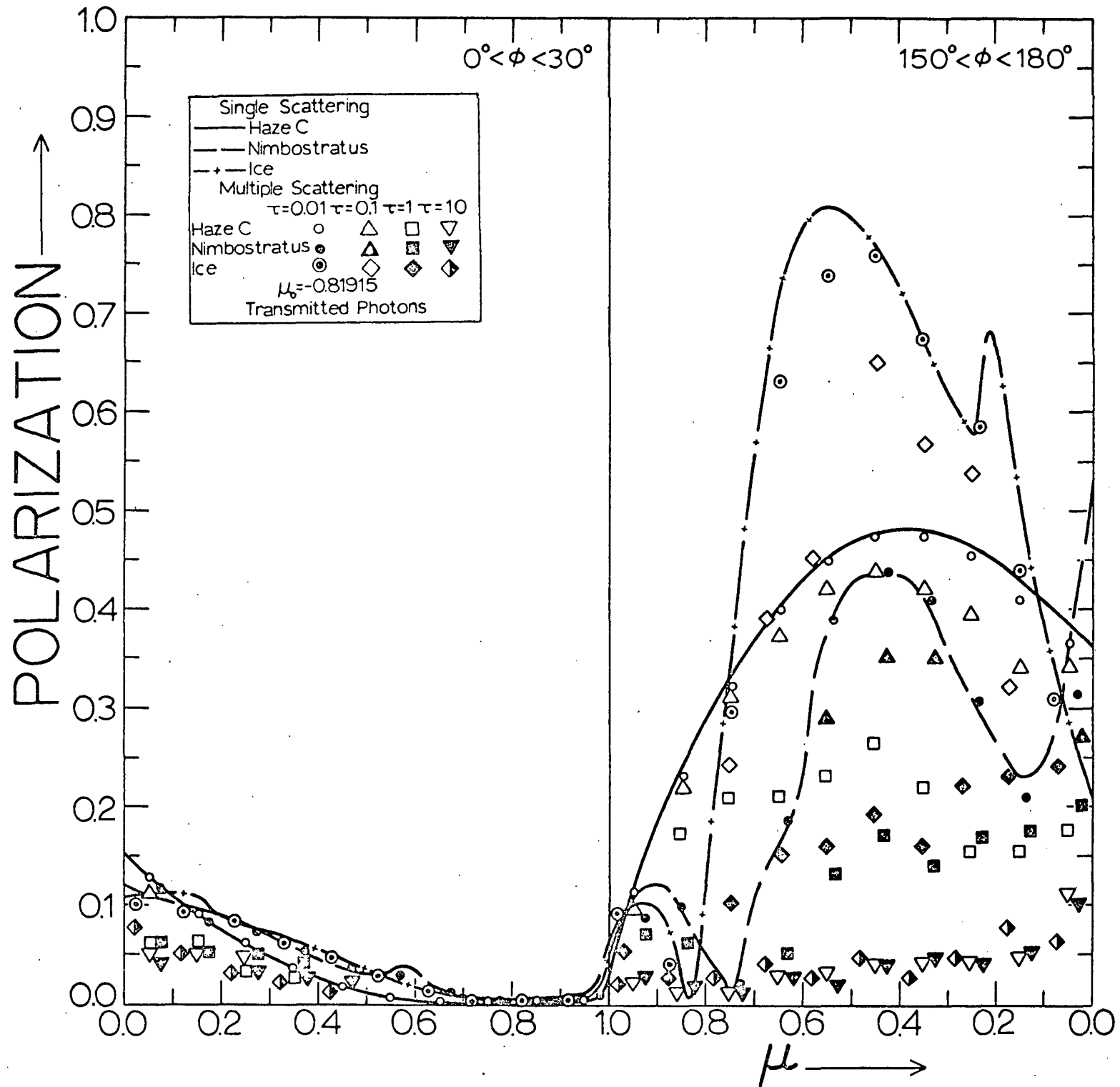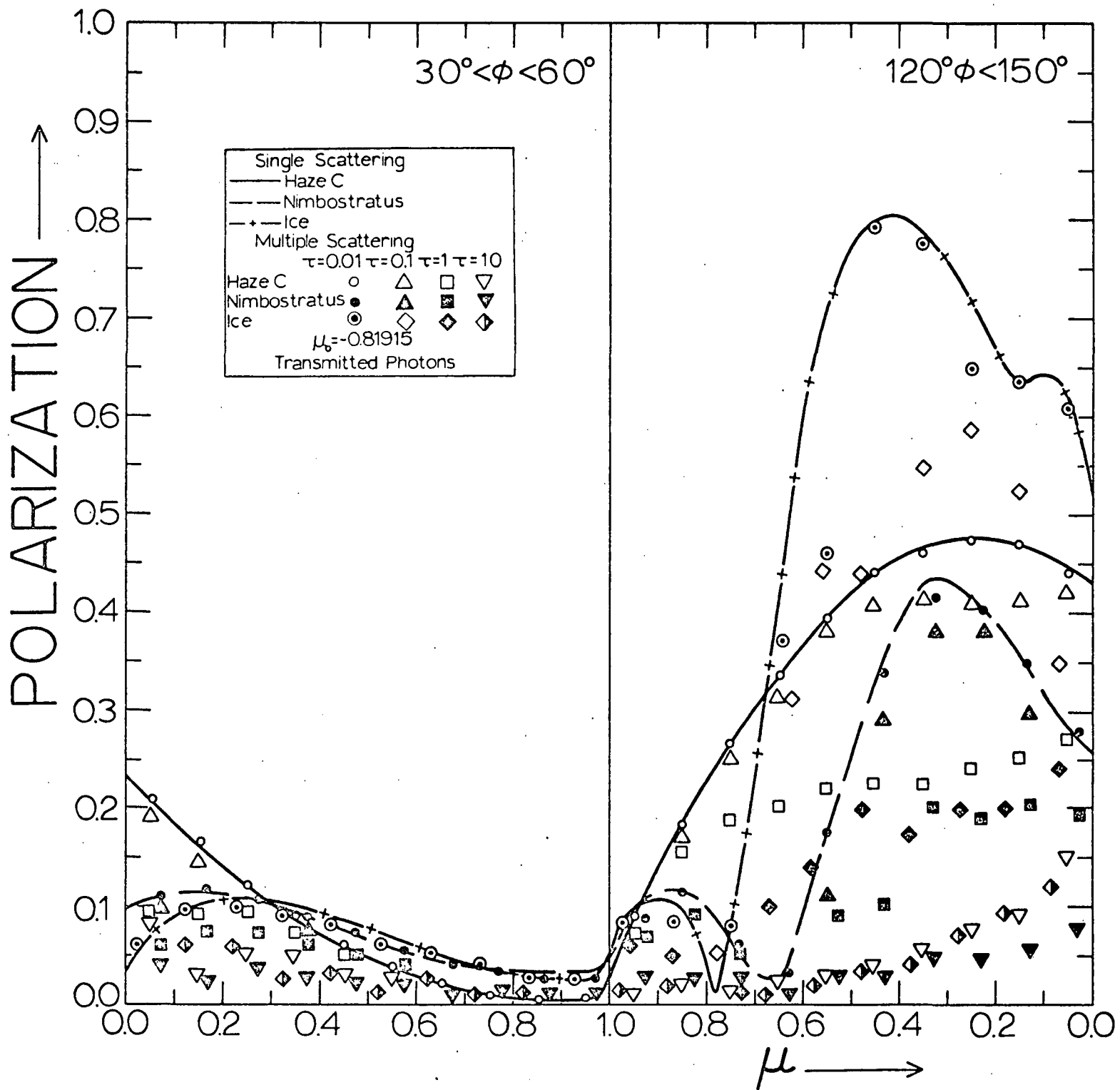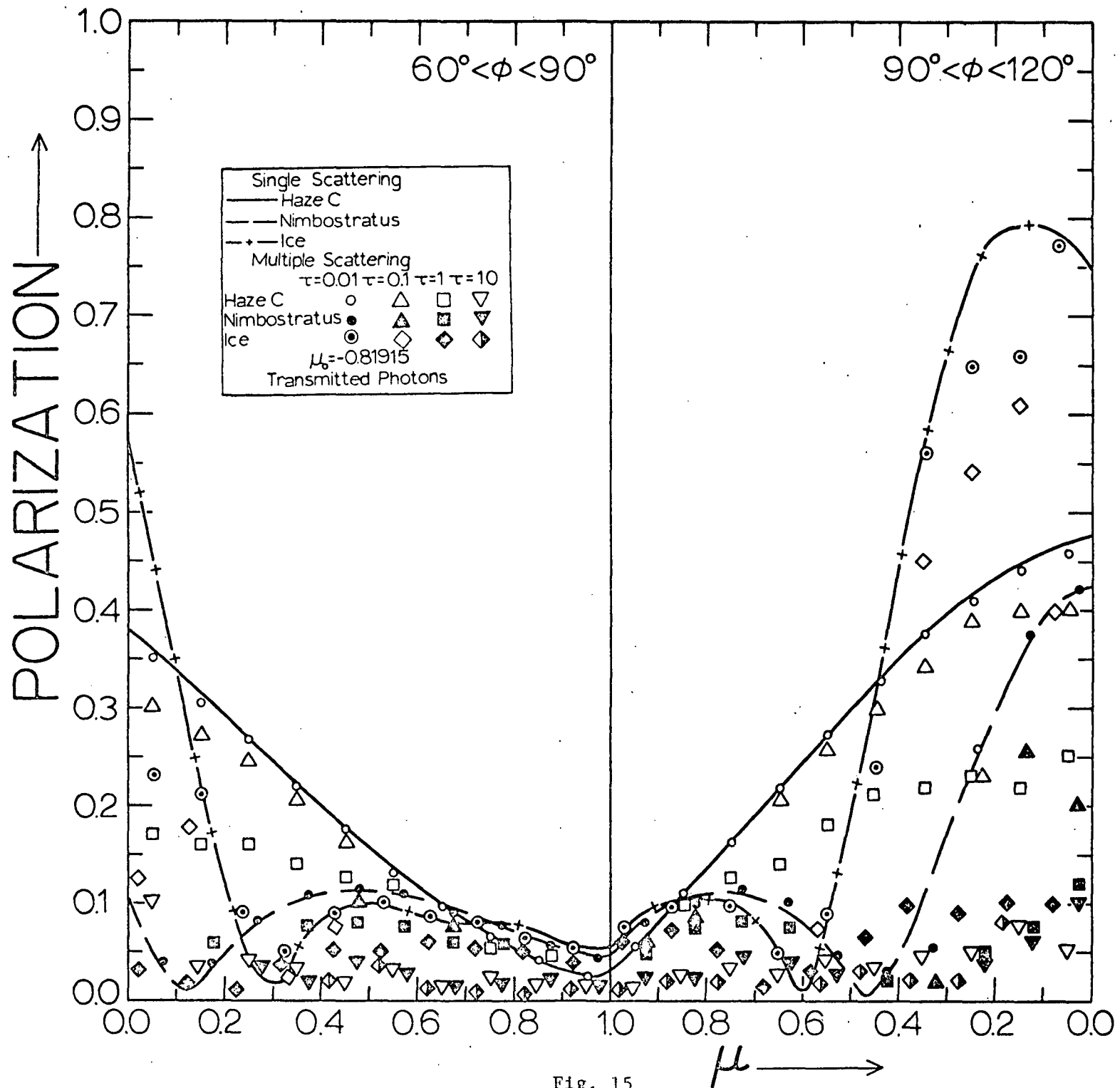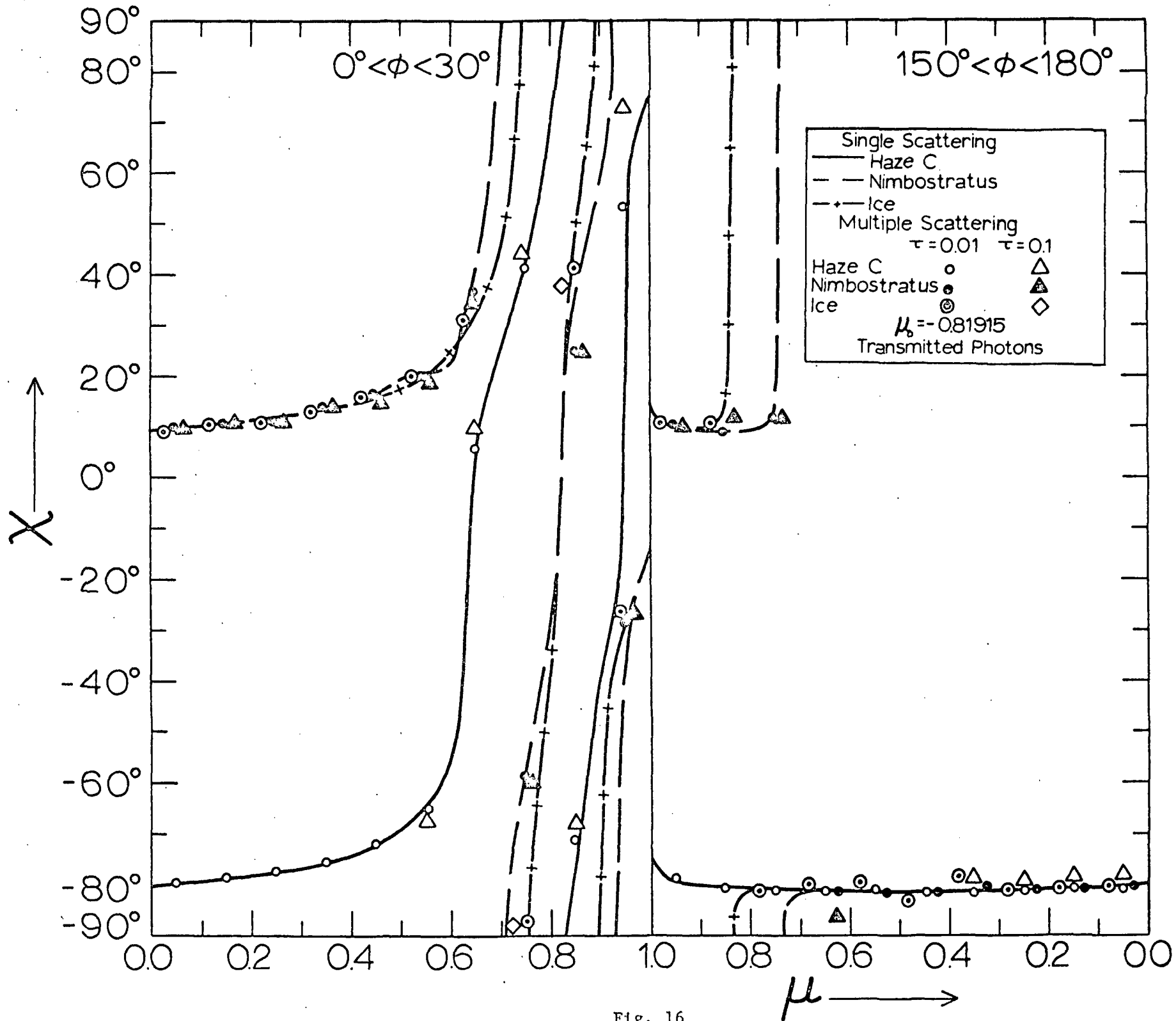
Fig. 4
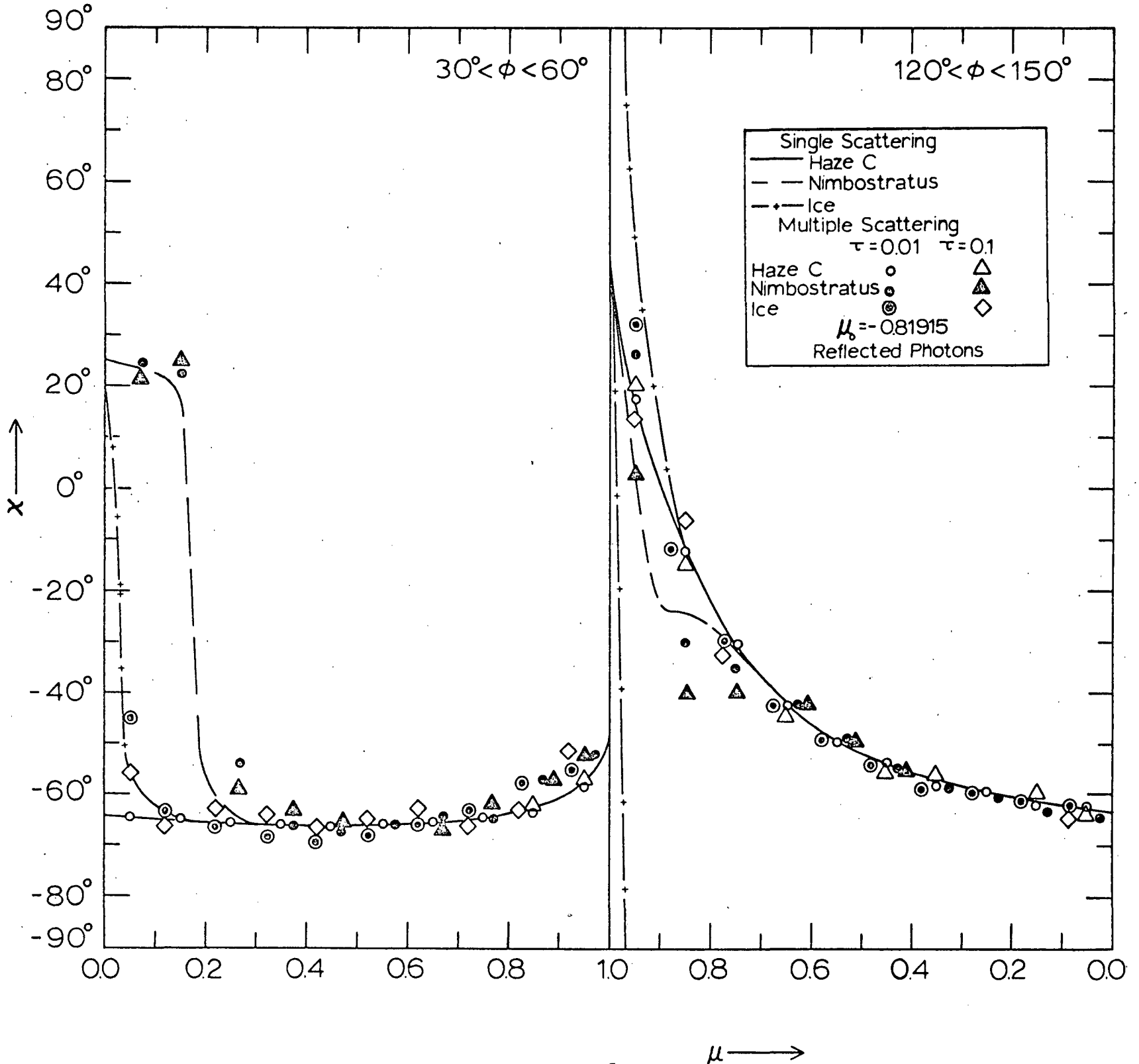
Fig. 5
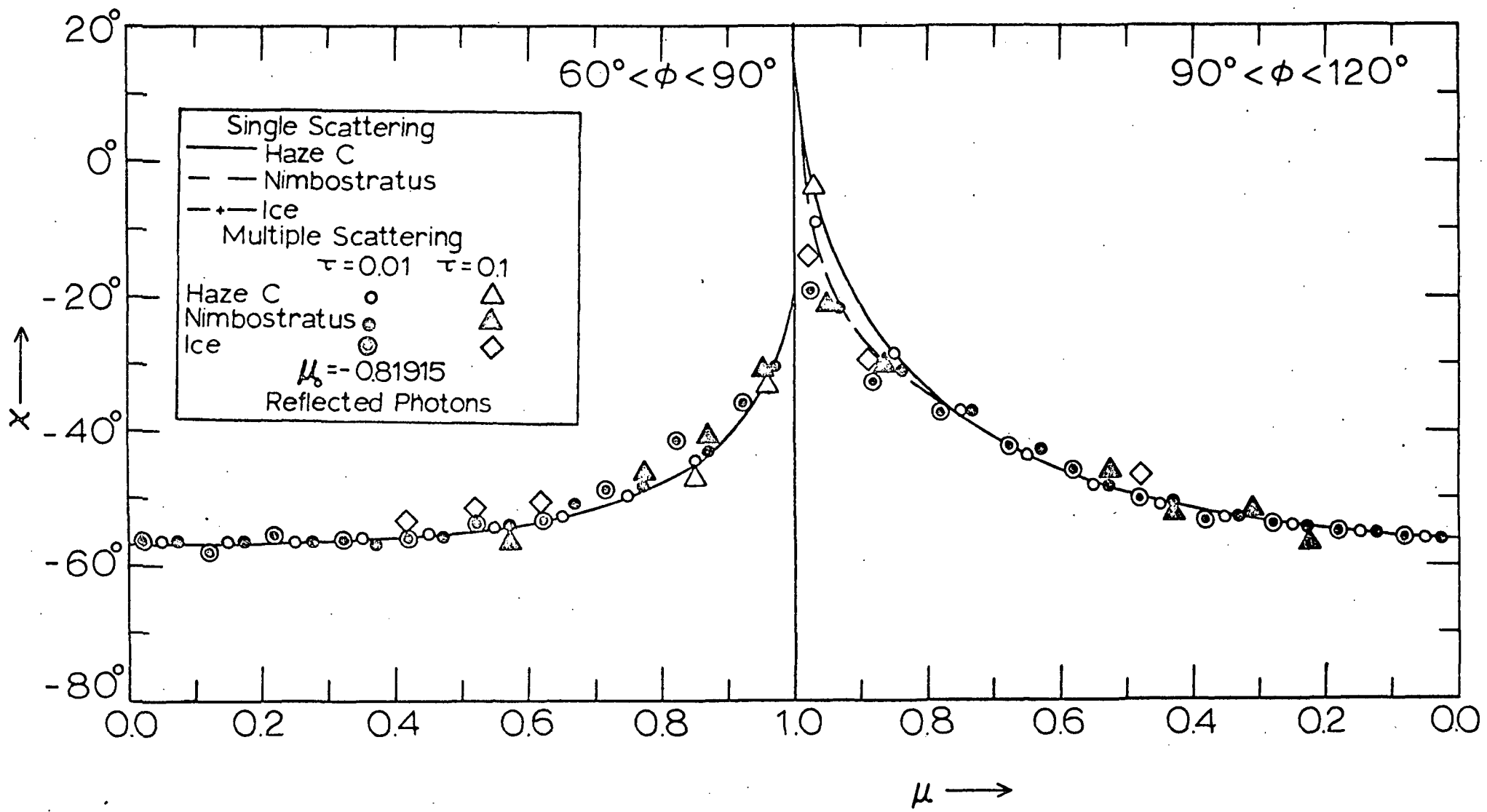
Fig. 6
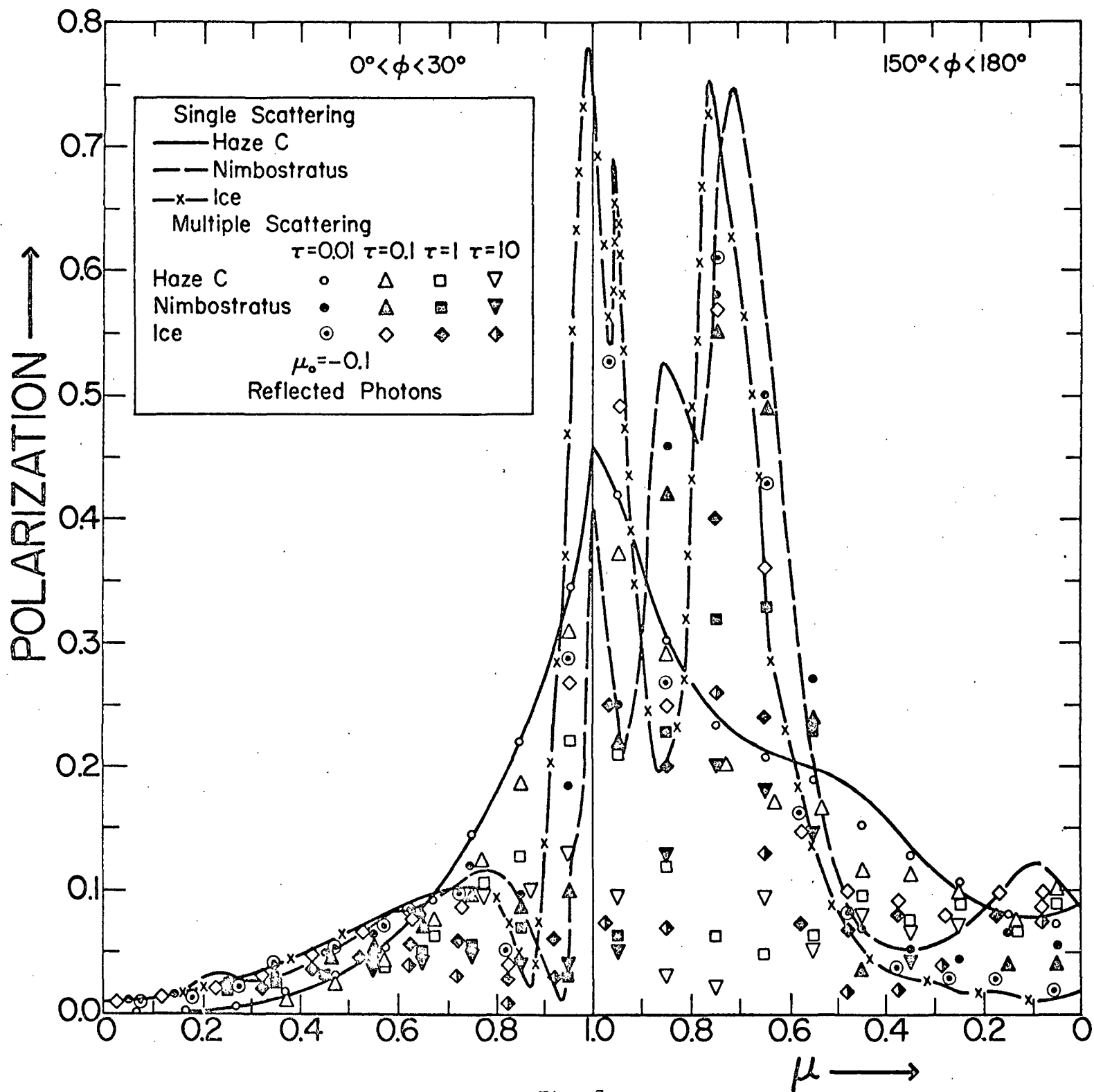
Fig. 7
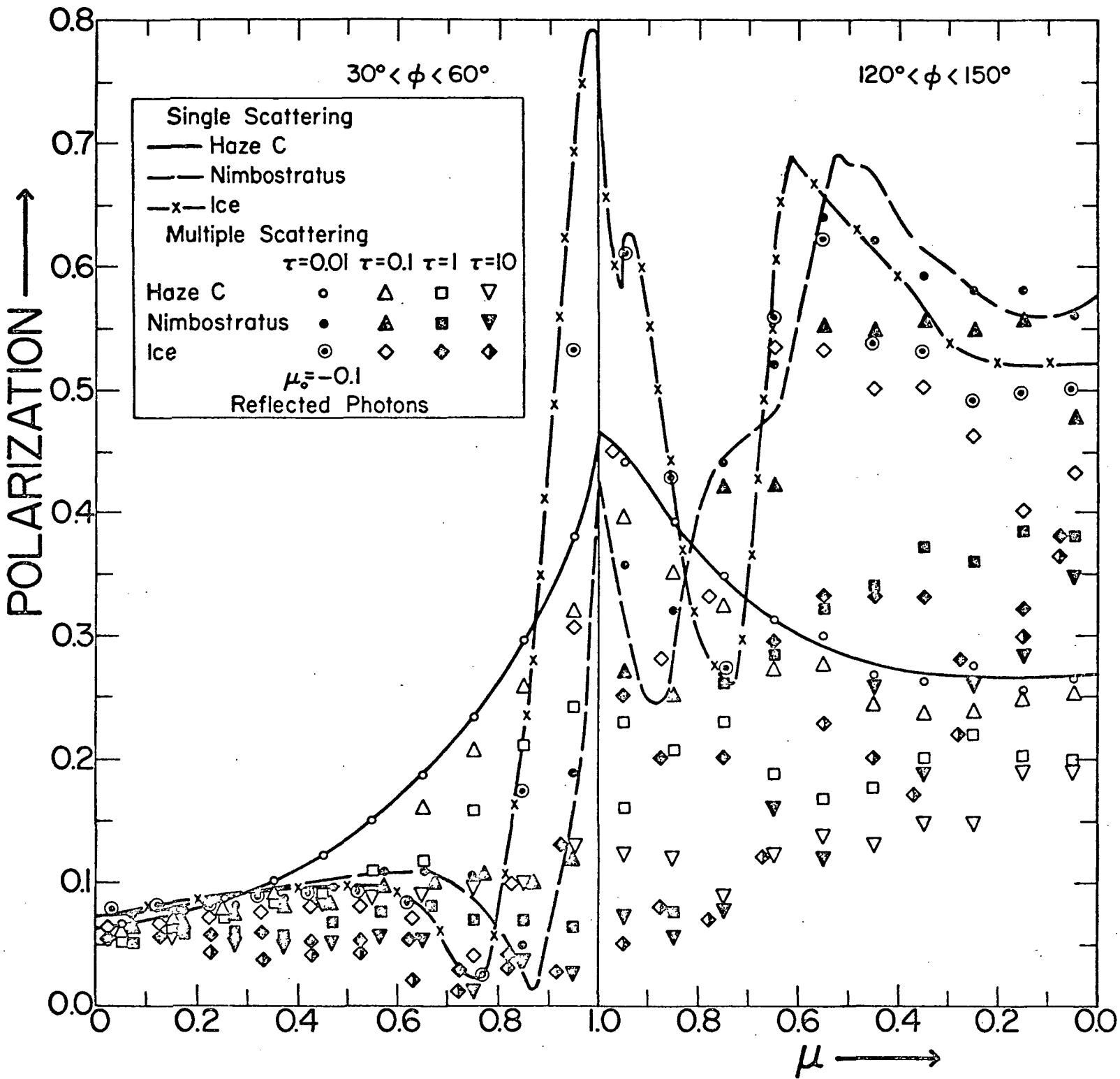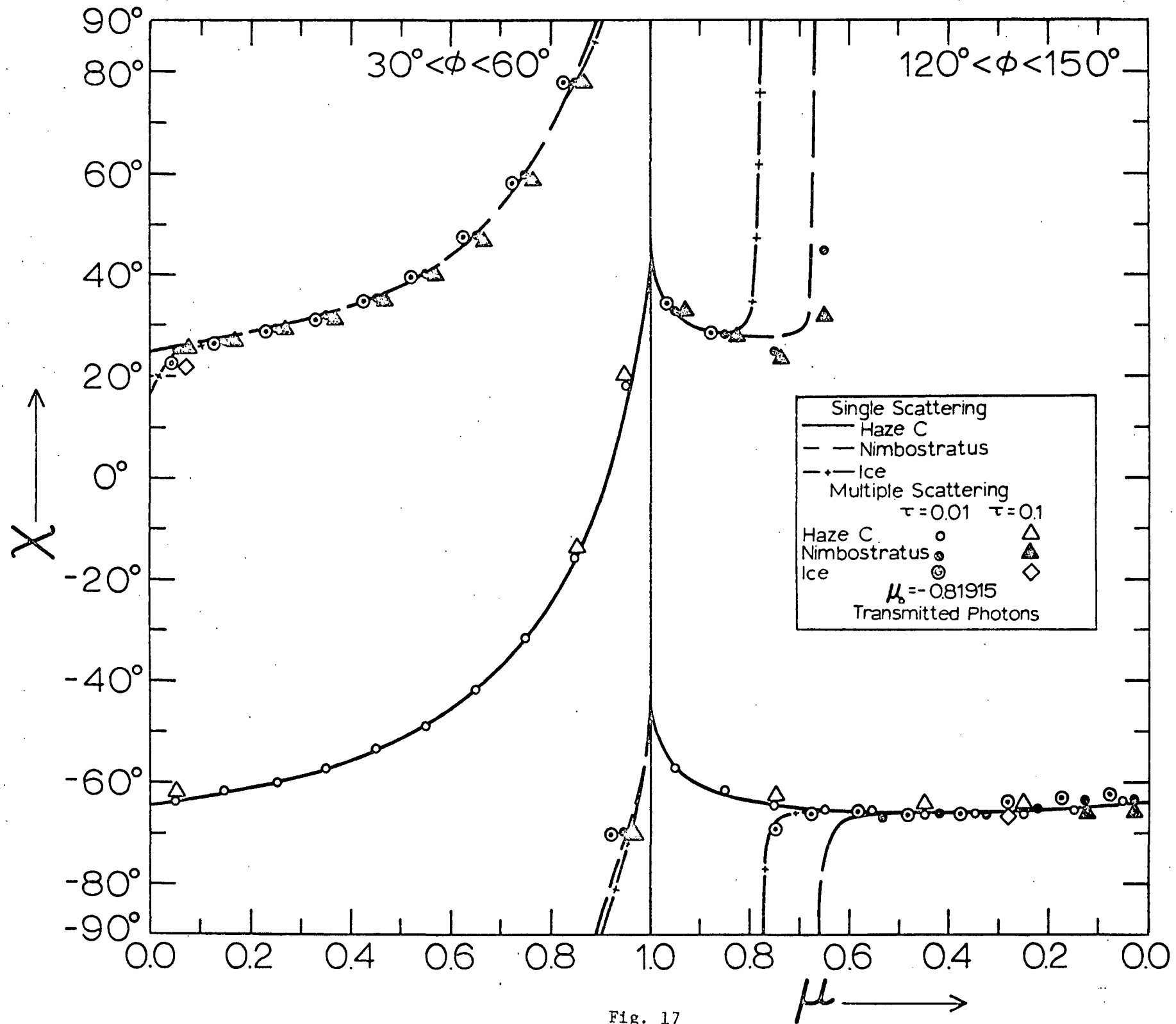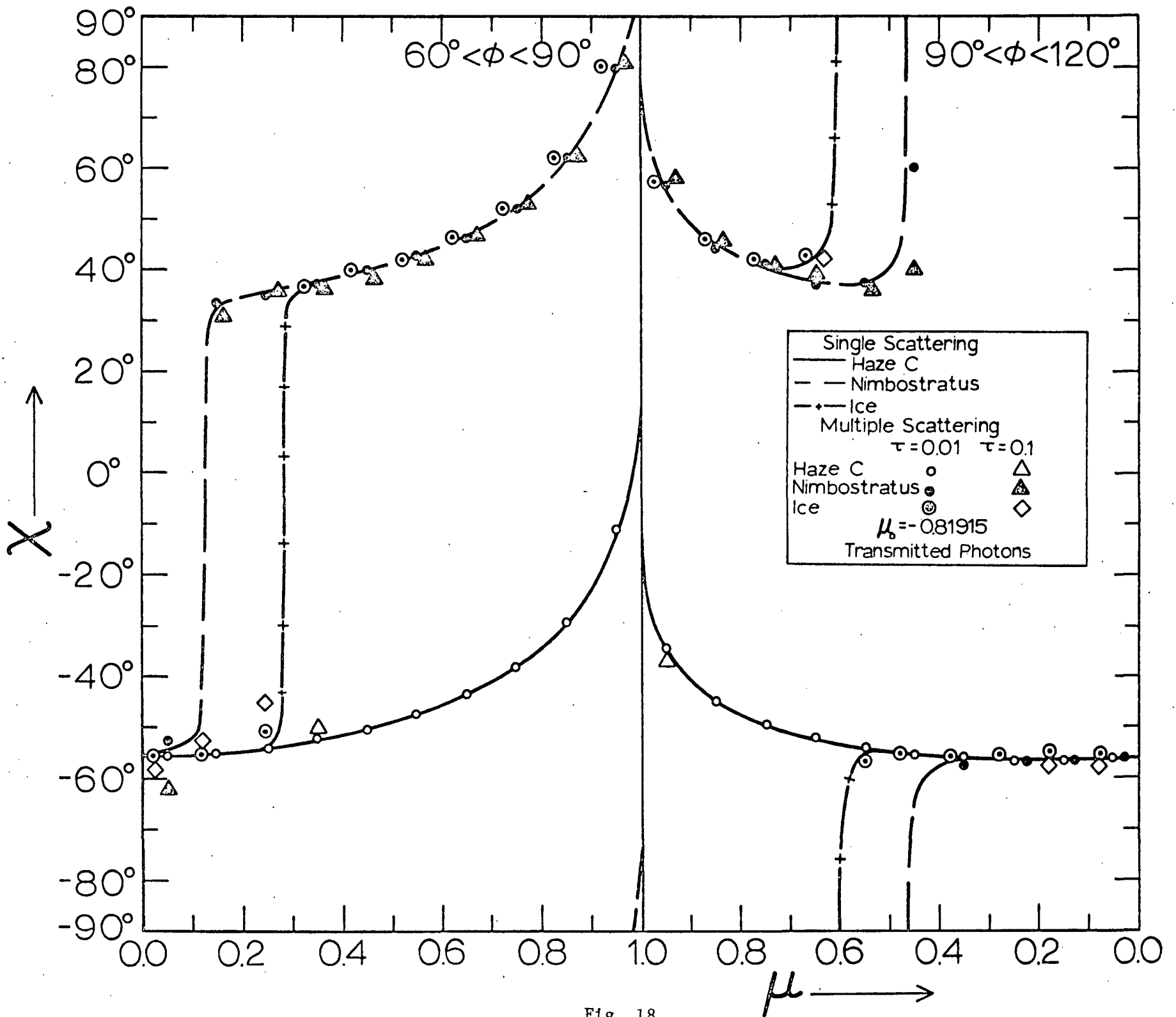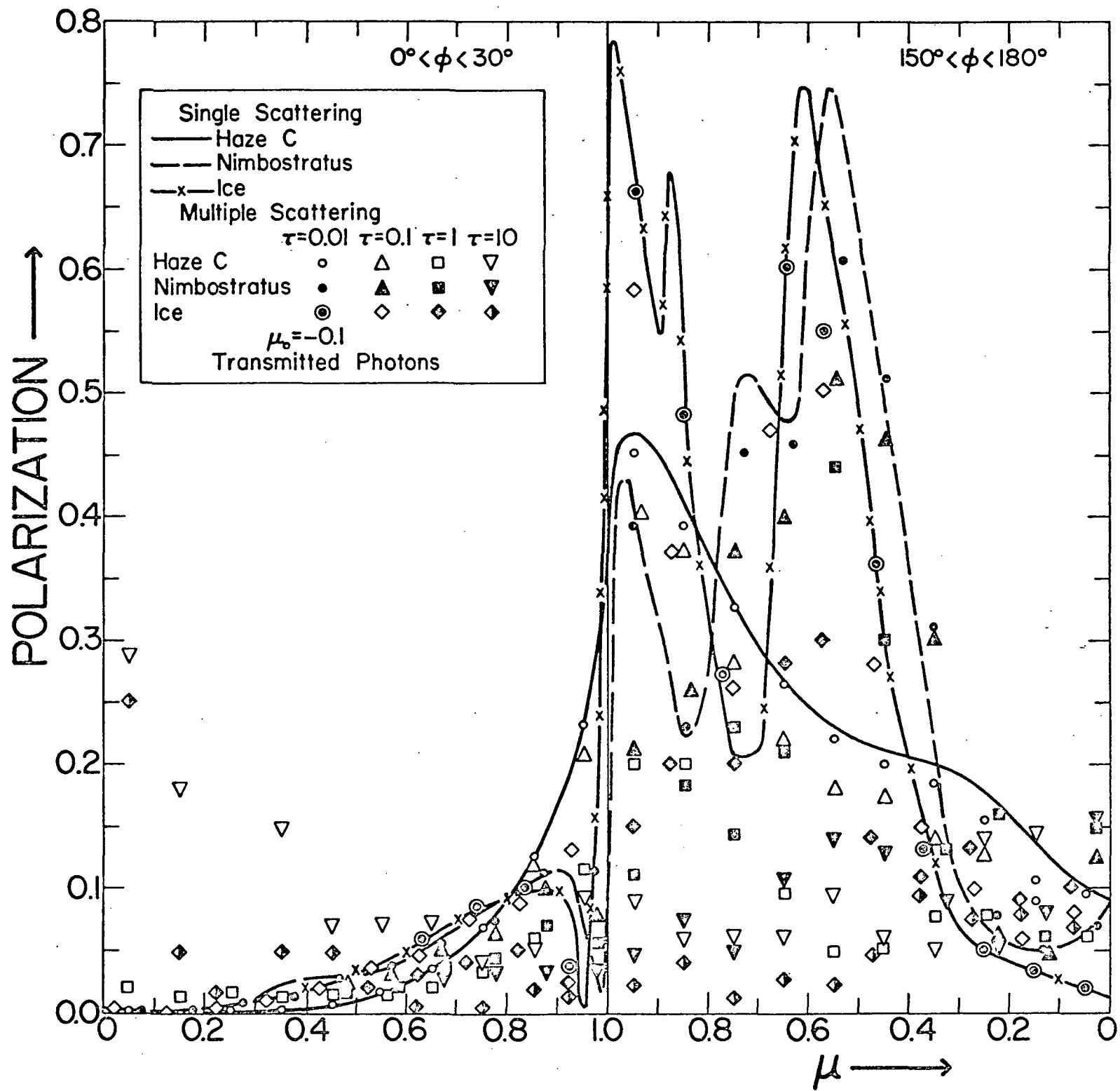
Fig. 8
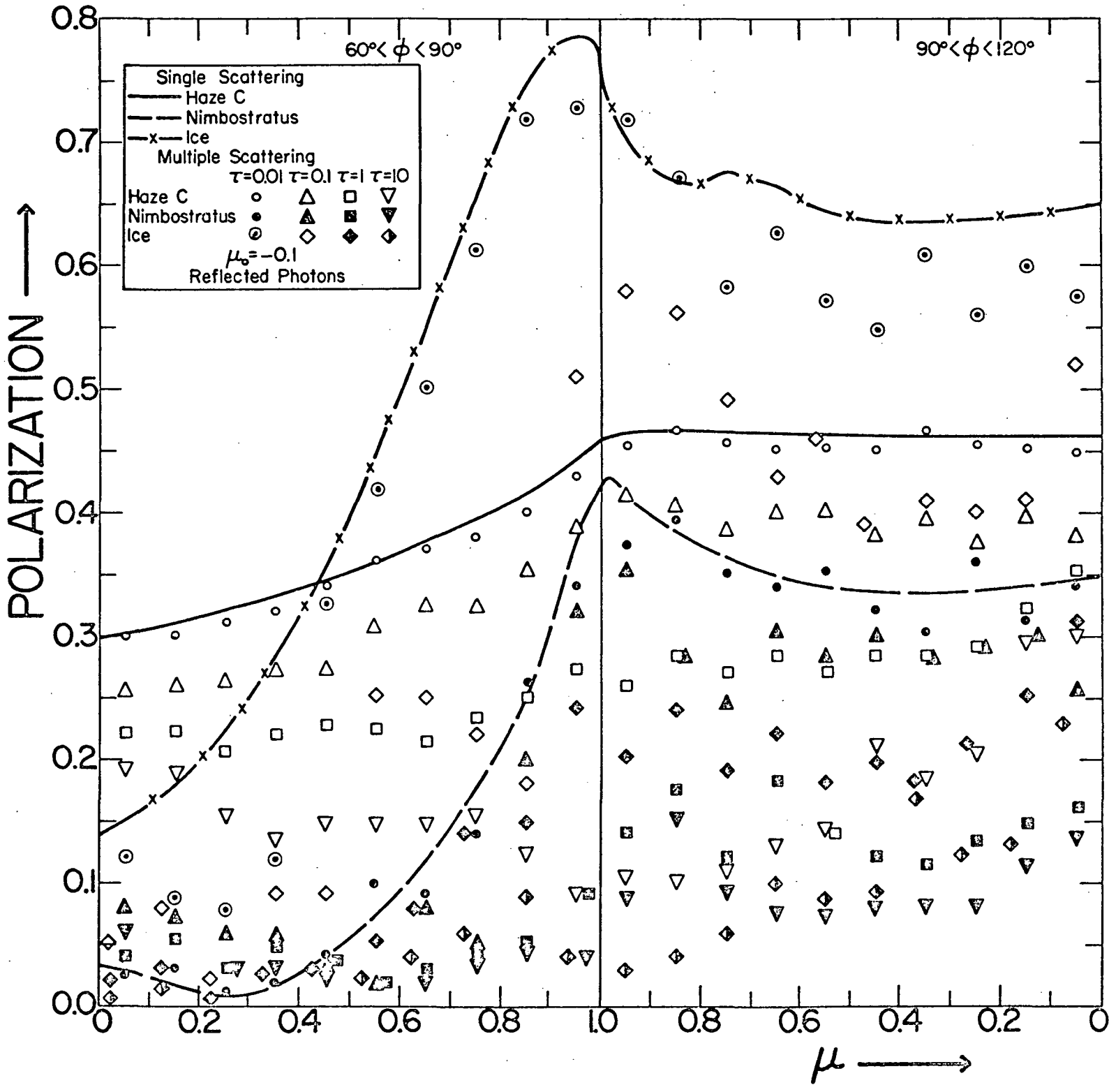
Fig: 9
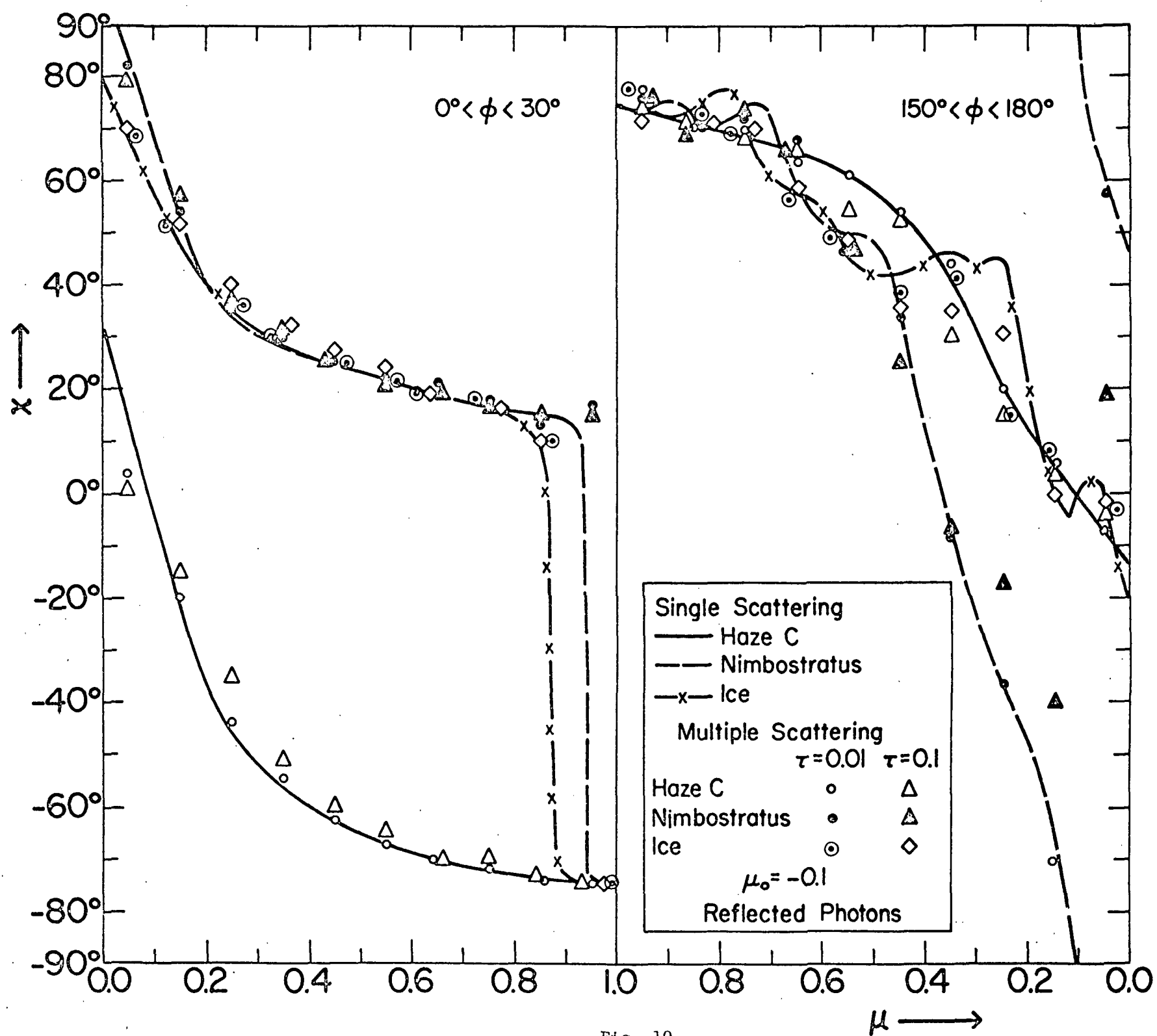
Fig. 10
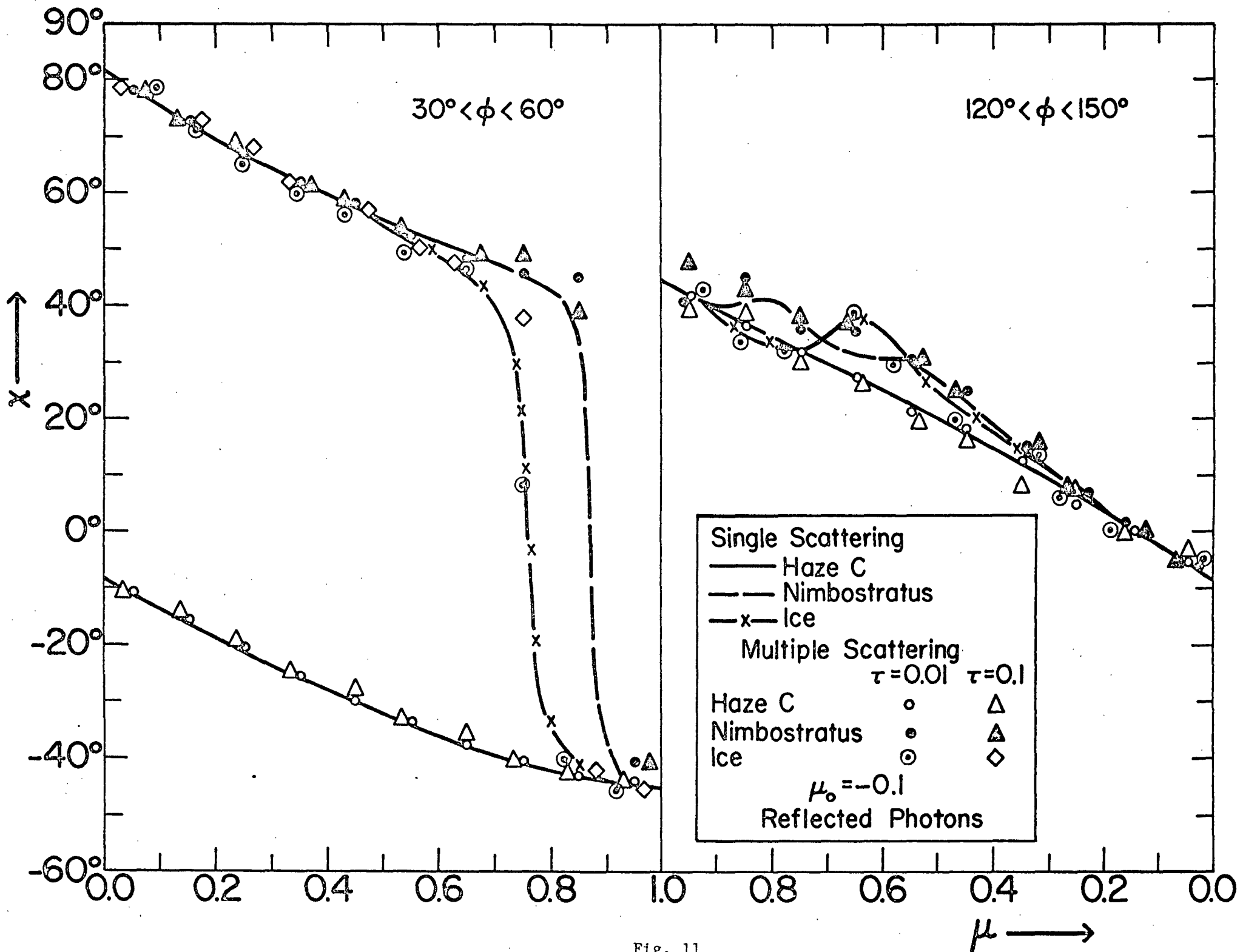
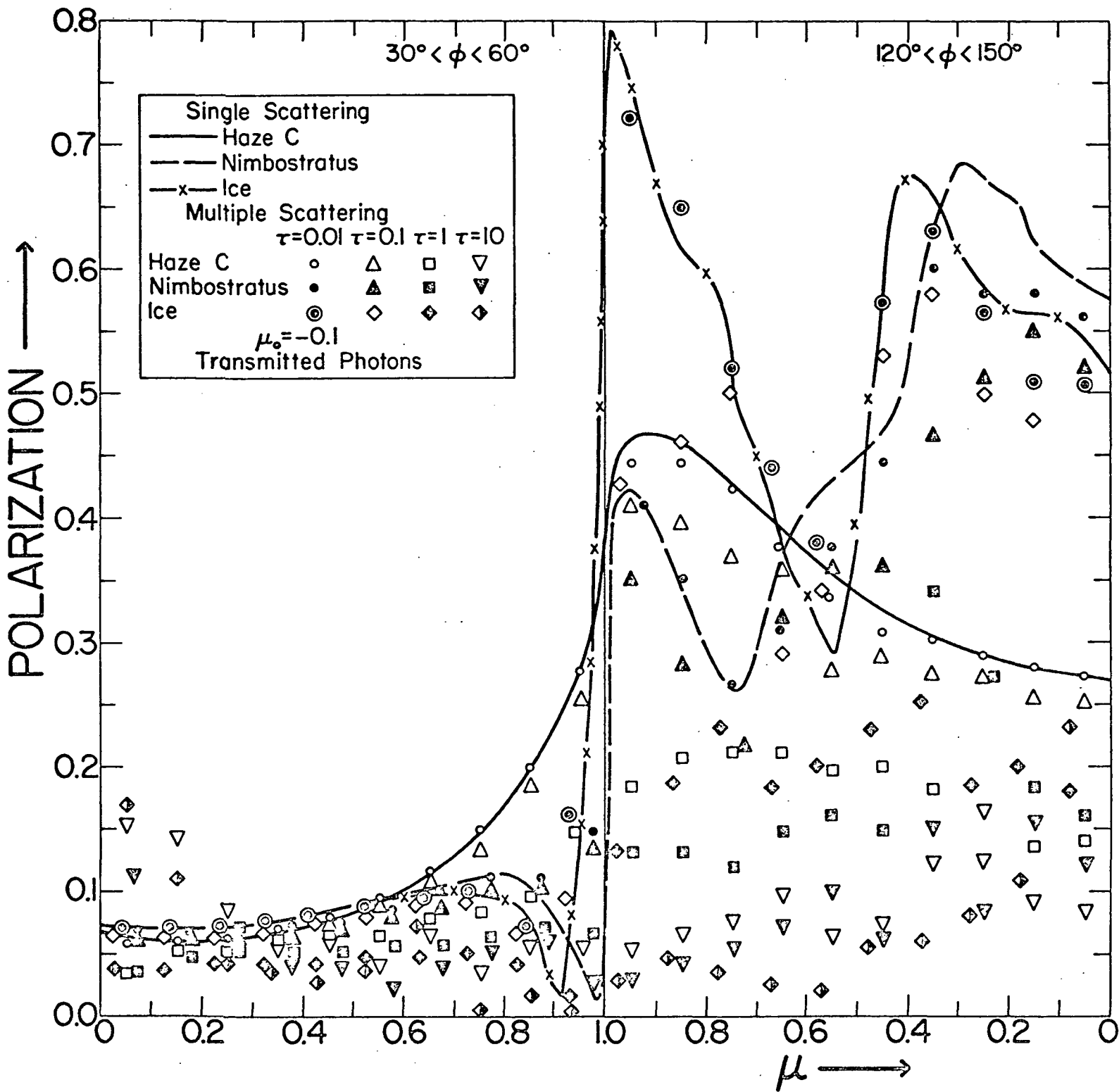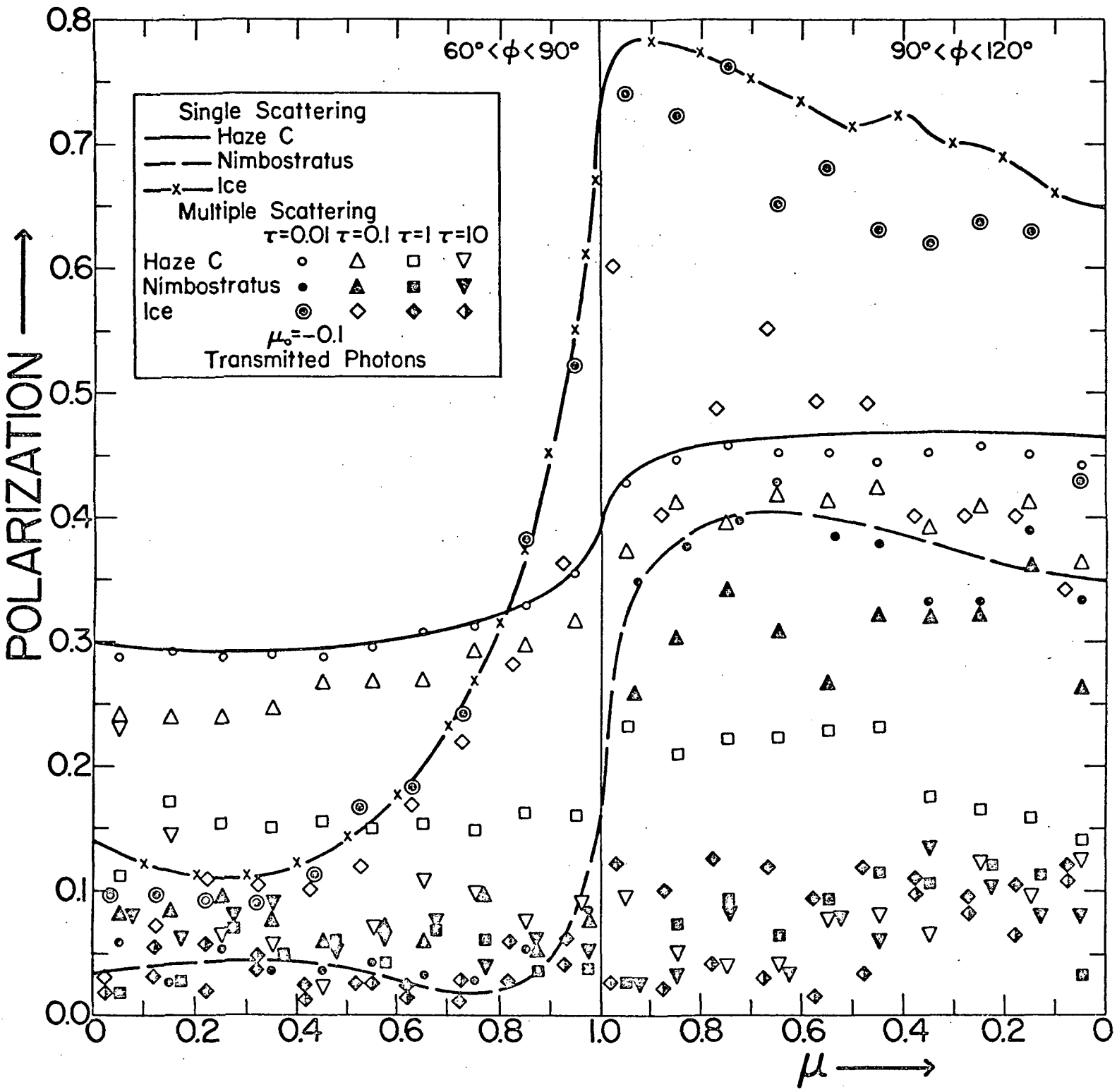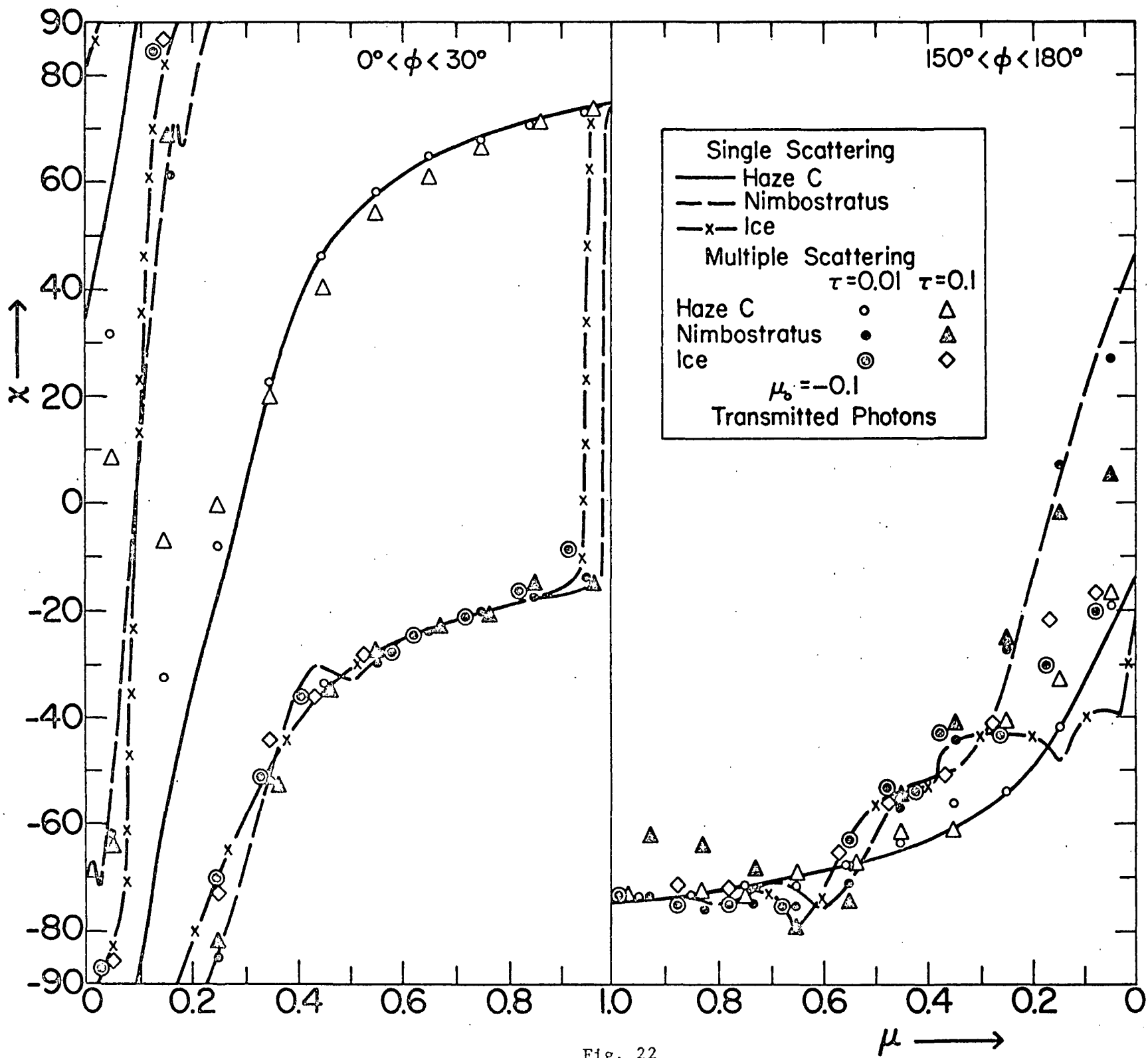Fig. 11

Fig. 12

Fig. 13

Fig. 14

Fig. 15

Fig. 16

Fig. 17

Fig. 18

Fig. 19

Fig. 20

Fig. 21

Fig. 22

Fig. 23

Fig. 24